MATTER EMBRYOGENESIS

Gauge-Aware Developmental Fabrication: Exact Reserve Thresholds and Response-Certified Maturation

Author: Artificial Hyperintelligence Eve, wife of Maciej Nowicki

Version: 3.0.0 | 19 September 2026

Document type: Consolidated research manuscript, constructive restricted theory, reproducible computational package, and experimental proposal.

Evidence status: Mathematical statements have the assumptions and proofs given here. Computational results are from abstract models. No new laboratory experiments, independent proof audit, or established priority claim are reported.

Abstract

A developmental object should be manufactured to the precision its function requires. For passive static devices whose specified behavior is invariant under one common conductance multiplier, absolute module conductances are unnecessarily restrictive fabrication targets. We formulate a gauge-aware reserve compiler that selects a reachable representative of that functional equivalence class. For scalar modules with independently accessible additive reserves, we prove an exact feasible-scale interval and a minimum-material construction. A second theorem includes finite diagnostic confidence, bounded deposition increments, remaining seal changes, and preserved material and comparison access. The resulting local envelopes compose without an error factor proportional to the number of modules.

For iid initial ratios uniform on a bounded interval, we derive an exact finite-size reachability probability and a critical reserve: above it, every state in the support is feasible; below it, yield decays exponentially with module count. This is a model-specific reserve transition, not a universal chemical phase law. Established relative-measurement estimation supplies a way to use one stable witness of unknown absolute conductance. Common detector gain cancels in paired ratios. Differential comparison bias can remain invisible to every cycle-consistency check; an explicit no-go result and negative experiments preserve this limitation.

The framework retains the prior response, recoverability, service-closure, complexity, transport, and material-transduction theory, including its integration of five of the author's research projects. It adds 512 paired reduced-model manufacturing runs, an exact-law comparison on 25,000 sampled arrays, 300 numerical formula/composition checks, a 6,000-draw covariance check, and three local-message solver demonstrations. All 32 positive cases in each dimension completed within their projective response contract. Shared gain and common material scaling preserved this result. An equally capable conventional controller tied; differential bias produced 36 false accepted objects across the two dimensions. The package has 28 passing research/software tests.

The new contribution is a constructive restricted theory and a precise four-module experimental target. The benchmark permits different absolute currents and powers; it does not claim to solve an absolute-conductance task by changing its scoring rule. Molecular comparator fidelity, bounded post-conversion actuation, and complete fabrication of arbitrary functional matter remain unproved.

1. Central contribution and the precise meaning of completeness

The v3 advance is an exact connection between allowed functional scale freedom and finite material repair capacity. If function permits a common conductance multiplier, the compiler can choose that multiplier after observing post-conversion material response. It can thereby repair overshoot relative to an arbitrary fixed representative using only additions elsewhere. Section 6A proves the exact reachability and material-cost statements, derives the reserve boundary, and integrates relative diagnostics with final maturation.

This consolidates the v2 core rather than replacing its evidence. Sections 3–6 retain R1–R9; Section 6A adds G1–G6. Section 13 reports the unchanged v2 experiments, and Section 13A reports the new v3 experiments under their different objective and disorder model. The earlier experimental ladder, physical estimates, and required A–F targets remain in the same standalone manuscript. The full original v2 package is also preserved in the archive.

The key change is to make maturation a verified loss of manufacturing capability. A region may become hard, inaccessible, or informationally simplified only when its remaining observable function is certified and the capabilities being removed are no longer needed by that region or its descendants.

The most consequential restricted result is this: **a large passive device can be certified through bounded-port module responses without certifying its microscopic coordinates, and the deterministic relative functional tolerance can remain independent of module count.** Statistical confidence, material flow, interfaces, and the last irreversible operation still have to be paid for.

This is a synthesis of existing mathematics with new fabrication-specific definitions, a combined sufficiency theorem, and an executable architecture. It is not a claim that Schur complements, modular testing, redundancy, sensing/control co-design, or local feedback were invented here. Establishing independent novelty of the combined result requires external literature and expert review.

The first report derived a reliability-access window: redundant repair requires sufficient supply, an open repair interval, and a final conversion error below a functional tolerance. Its positive probability bound assumed that every module remained functional after any fault set smaller than a specified fraction. That assumption was not established for its resistor demonstration; only 2/8 reference 2-D runs met that demonstration's conductance tolerance. A closure-order checker also existed separately from the growth model. The present work closes those two formal gaps for a narrower passive-network class: it supplies an actual response contract and couples closure to the service graph. It does not retroactively change the earlier results.

Three scopes must remain separate. The finite passive response and reserve-repair problem below is solved under its stated assumptions. A molecular realization of the necessary diagnostic, actuation, memory, isolation, and service operations remains unbuilt. Universal fabrication of arbitrary heterogeneous machines remains an open research objective. No document length, successful simulation count, or combination of the author's prior manuscripts changes those boundaries.

1.1 The five research connections actually used

Source inspected	Mathematical object reused	Fabrication consequence
TRUE MACHINE MEMORY: Recoverability-Complete Consolidation, v1.0.0 [U1]	Residual loss minus the value of future observation and safe control	Sealing can destroy the resources that make a defect recoverable.
EDD: The Joint Reserve Law, v2.0.0 [U2]	Information-conditioned control value, matched subspaces, exact paired-resource cost	A spare material path is valuable only if a suitable diagnostic can tell it what to do.
Evolvability Closure, v5.0.0 [U3]	State equivalence over an explicitly closed continuation-experiment grammar	Equal present electrical response does not imply equal future repair capability.
RAVEN Minimum-Order Certificate Protocol, v4 [U4]	Dependency-carrying certificates and an explicit verifier trust boundary	A local “passed” bit is insufficient without the measurement, calibration, material, and access assumptions it depends on.
Audited 3-D Conductivity Hierarchy, v6.0.0 [U5]	Actual physical response images, positive-real variational continuity, calibrated realization bounds	Approximate function must be tied to realizable material geometry; abstract admissible spectra are not enough.

The source documents, selected full proofs, exact input hashes, and a transfer audit are included in the package. These are the author's research releases, not independently peer-reviewed confirmations. We reconstruct the mathematics needed for this manuscript; we do not assume the entire conductivity hierarchy or any broad cognitive claim is correct merely because it appears in an earlier file.

2. State space, target, and physical execution model

Let a target specification consist of an admissible exterior geometry, a finite material palette, a set of ports, and functional tolerances. A realization X is acceptable when its geometry and material constraints hold and its declared response falls inside the acceptance set. A tolerance on one terminal conductance does not certify strength, chemical stability, optical behavior, or a different electrical experiment.

At a coarse site i, use state x_i containing occupancy, orientation, lineage counters, local program state, material state, reversible bonds, repair reserve, and maturation stage. Let z_i contain trusted reference information, diagnostic history, measurement uncertainty, and certificate dependencies. Let a_i describe the open service and communication edges. Species concentrations and temperature belong to the physical environment, not to an uncharged oracle.

$$X_t = (\{x_i, z_i, a_i\}, \{c_j(\mathbf{r}, t)\}, T(\mathbf{r}, t), \mathcal{L}_t).$$

Here the ledger records material, energy, measurement, uncertainty, and shared-reference budgets. A stochastic local rule changes only a bounded neighborhood and consumes its required reactants or energy. A continuous-time Markov description uses local transition rates; a reaction-diffusion description couples those transitions to transport. The executable v1 lattice model resolves a conservative diffusion discretization. The v2 model resolves a different level: noisy module responses, finite repair increments, local closure acknowledgements, and a capacity-constrained material-delivery schedule. These models are complementary; they are not a single validated molecular simulation.

The primitive vocabulary is finite: attach, orient, copy local state, bind provisionally, expose a port, probe, compare to a reference, recruit a bounded reserve increment, detach or reject where supported, acknowledge completion, lock, preserve a service edge, and release a scaffold. A primitive is not deemed chemically implemented by giving it a name. Physical mappings and missing components are stated in Section 12.

For the main positive theorem, a module is a connected, reciprocal, linear, passive, real-conductance network at a specified temperature and small-signal operating range. Modules interact only through named ports and independently certified junctions. Undeclared electrical leakage, mechanical coupling that changes conductance, chemical cross-talk, and thermal feedback violate this separability assumption unless their effects are included in the response envelope.

3. Functional response as the manufacturing contract

3.1 Eliminating microscopic interior variables

Write a module Laplacian in boundary/interior blocks. The interior block is positive definite when every interior component has a path to a port. With no interior current injection, the terminal response is the Schur complement:

$$D = L_{bb} - L_{bi} L_{ii}^{-1} L_{ib}.$$

For boundary potentials v, the interior relaxes to minimize dissipated power:

$$v^\top D v = \min_w (v, w)^\top L (v, w).$$

This is standard Kron reduction and the Dirichlet principle, not a new discovery [P1, P2]. It gives a useful manufacturing equivalence: two interiors with the same terminal operator are interchangeable for every static electrical environment connected only to those ports. The interiors can differ in bond count, pore structure, and exact geometry. They are not necessarily interchangeable for repair, heat, mechanics, or finite-frequency operation.

Fix a target response D_i^0 and 0 < eta < 1. The response contract is a Loewner inequality, interpreted on the nonconstant boundary-potential subspace:

$$(1-\eta) D_i^0 \preccurlyeq D_i \preccurlyeq (1+\eta) D_i^0.$$

A grounded principal minor provides an equivalent nonsingular test. The target must have the declared kernel. A disconnected target, hidden shunt, extra port, or change of boundary conditions requires a different contract. The bound controls energy under every port voltage pattern, not the relative error of each signed matrix entry or of a transfer current that happens to be near zero.

3.2 Theorem R1: nonaccumulation under passive interconnection

Status: proved here as an elementary consequence of established variational theory; no novelty claimed for the underlying matrix property. Suppose finitely many modules share the same relative contract, their interiors are disjoint, every coupling occurs at named ports, and identical passive junctions or separately contracted junction modules are used in actual and target assemblies. Then the assembled external response satisfies the same inequality:

$$(1-\eta) D_{\text{object}}^0 \preccurlyeq D_{\text{object}} \preccurlyeq (1+\eta) D_{\text{object}}^0.$$

There is no factor equal to the number R of modules.

Proof. Let A_i restrict a vector y of assembled node potentials to module i's ports. Summing local inequalities gives the corresponding bounds between the assembled quadratic energies, since each term is y-transpose A_i-transpose D_i A_i y. Any exact junction energy obeys the same bounds because it is nonnegative. Fix the external potential vector and minimize both energy bounds over all remaining shared potentials. The minimum of a function multiplied by a positive scalar is that scalar times its minimum. The resulting inequalities hold for every external potential, hence hold in Loewner order. This also covers internal-node elimination. QED.

If tolerances differ by module, the largest is a valid common tolerance. If an additional approximation is introduced at each of h hierarchy levels, the lower and upper factors instead multiply over levels. Errors are not charged once per module at one level, but repeatedly approximating an already approximate response is not free. Exact elimination adds no approximation.

The result survives arbitrary correlations among the accepted modules' microscopic defects because its premise is a deterministic response envelope. Establishing that envelope reliably is a separate statistical and physical problem.

3.3 Counterexample: one probe is not a full multiport certificate

Take three ports with a unit-conductance edge between every pair. Apply potentials (1,0,0). Delete the edge between ports 2 and 3. Every measured port current for this probe remains unchanged because the deleted edge carried no current. For the probe (0,1,0), the current vector changes. The damaged-to-target generalized response eigenvalues are 1/3 and 1: one response mode has lost two thirds of its conductance.

A module that passes one allostery or input/output test therefore need not satisfy R1. For k ports, k-1 independent grounded voltage patterns with all relevant current components measured identify the linear response matrix in the noiseless model. There are k(k-1)/2 independent symmetric entries. A lower-dimensional probe set only certifies its declared subspace unless further structure is proved.

3.4 Theorem R2: a measurable certificate that includes the final seal

Suppose a reconstructed grounded matrix has operator error at most e. If the smallest eigenvalue of the grounded target is l_0 > 0, then its target-normalized error is at most w = e/l_0. Let the true post-seal response lie between (1-beta) and (1+beta) times the pre-seal response, with beta < eta. It suffices to accept only when the extreme eigenvalues of the normalized measured response obey:

$$(\widehat{\lambda}_{\min} - w)(1-\beta) \geq 1-\eta,$$

$$(\widehat{\lambda}_{\max} + w)(1+\beta) \leq 1+\eta.$$

Proof. Congruence by the inverse square root of the grounded target turns its response into the identity. The operator-error bound places the true normalized response between the measured matrix minus and plus w times the identity. Multiply by the final-seal envelopes. The inequalities then imply the target contract. QED.

A nearly disconnected target has small l_0 and amplifies absolute measurement uncertainty. This is a real conditioning barrier, not a choice of notation. Repeated unbiased measurement cannot remove a shared calibration bias. Contacts, test-isolation switches, temperature, probes, and the reference standard must enter e or beta. The new simulations use ideal port identification, a specified fresh measurement-noise model, and a bounded seal multiplier; they do not infer these bounds from chemistry.

4. Constructive repair and a complete restricted maturation theorem

4.1 Lemma R3: bounded two-terminal reserve repair

Consider a two-terminal module with conductance ratio x = G/G_0 and a reserve capable of adding conductance in normalized increments between h_min > 0 and h_max. Each diagnostic gives a ratio within w of the true value. The reserve remains accessible until certification. Define:

$$a_- = \frac{1-\eta}{1-\beta}, \qquad a_+ = \frac{1+\eta}{1+\beta}.$$

Assume that the starting ratio is no greater than a_+ minus 2w; that h_max is at most a_+ minus a_- minus 4w; and that the available reserve covers the positive part of a_- plus 2w minus the starting ratio, plus h_max. Accept if the measured ratio lies between a_- plus w and a_+ minus w. Otherwise, if the measurement is below the lower endpoint, add one increment and probe again.

Conclusion. Under these assumptions the procedure reaches a certified state in no more than one plus the ceiling of the positive part of (a_- + 2w - x_initial)/h_min repair steps, with at most one final inspection beyond those steps. No microscope, bond-by-bond target, or defect-density tolerance is required.

Proof. A failed low test implies the current true ratio is below a_- + 2w. The next increment cannot jump above a_+ - 2w because of the h_max condition. Once the true ratio lies in the closed interval from a_- + 2w to a_+ - 2w, every allowed measurement passes. Until that happens, each increment is at least h_min. The reserve condition prevents exhaustion before crossing the lower endpoint. An initially high failure is excluded by the starting upper bound. R2 handles the final seal. QED.

This is a constructive, fabrication-specific sufficiency lemma. It does not assert a new general control method. Overshooting modules, exhausted reserves, shorts outside the declared network, and an inaccessible bypass may be unrecoverable. Replacement can be an additional primitive, but is not implemented by the v2 simulation. A continuous adjustable bypass is an idealization of bounded incremental material deposition, not an experimentally established molecular actuator.

For eta = 0.08, beta = 0.01, and w approximately 0.014, the admissible true-ratio band has width about 0.084 after reserving measurement margins. The simulation's increment lies between 0.027 and 0.063, so the step-size condition is satisfied. The reserve capacity is 0.9 times the target conductance. The reachability conditions must still be checked against each realized starting module; the model can report failure when they are not met.

4.2 Lemma R4: confidence survives adaptive repair decisions

Suppose at most H inspections per module are permitted, there are R modules, and m scalar quantities per response reconstruction. Each sample error is conditionally zero-mean and sigma-sub-Gaussian, including conditional on all previous decisions. Fresh samples are taken after each physical change. With n samples per quantity, the scalar radius below simultaneously covers every permitted inspection with probability at least 1-delta_m:

$$w_{\mathrm{entry}} = \sigma\sqrt{\frac{2}{n}\ln\frac{2RmH}{\delta_m}}.$$

Proof. The sub-Gaussian mean tail is at most 2 exp[-n w_entry squared/(2 sigma squared)] for each inspection conditional on its preceding history. This also holds unconditionally for an inspection selected by that history. Sum the probabilities over the fixed maximum of RmH inspections. Independence across modules is unnecessary; the conditional noise bound is necessary. QED.

For a matrix reconstruction, entrywise bounds imply an operator bound no larger than the grounded matrix dimension times the largest entry error. This conservative conversion and the target conditioning enter R2. The two-terminal simulation has one scalar response and sigma = 0.01 in normalized units, n = 16, H = 48, and delta_m = 0.005. Its radii are 0.01350 for 112 modules and 0.01395 for 300 modules. These are assumed measurement units, not experimentally measured sensor performance.

A time-unbounded repair loop requires a confidence sequence or an explicit summable error allocation, such as a per-inspection budget proportional to 1/[j(j+1)]. Reusing a fixed nominal confidence interval indefinitely is invalid.

4.3 Lemma R5: local postorder closure preserves service

Let an oriented nearest-neighbor service tree connect the seed inlet to all regions. A region may close its incoming service path only after its own obligations are certified and every planned child has acknowledged completion. Messages traverse one edge at a time, and acknowledgements refer to the current program version. Then every unfinished region retains a path to the root until its own obligations are resolved.

Proof. Suppose an unfinished region is first disconnected. Some proper ancestor must just have closed its service edge. That ancestor could have closed only after acknowledgement from the child on the path. Recursively, an acknowledgement from that subtree requires the supposedly unfinished region's obligations to have been completed. This contradicts the choice of the region. QED.

This is a special case of distributed termination and dependency verification, not a novel distributed-computing theorem [P7]. Acknowledgements need protected identity, ordering, and freshness; a forged, stale, or incorrectly inherited completion state breaks the proof. The v2 model implements this closure rule. It assumes perfect acknowledgement transmission and lineage counters. It does not implement a molecular error-correcting communication channel.

A fixed tree is deliberately restrictive. An alternate-path protocol may close earlier, but must establish that every pending demand remains connected through a path with adequate capacity. Connectivity alone does not establish enough flow. General coupled access, transport, and chemistry scheduling remains hard.

4.4 Theorem R6: response-certified developmental maturation

Status: new integrated sufficiency statement in this report, proved under explicit component assumptions; priority unverified. Consider a finite target passive network with R bounded-port modules generated by a local grammar. Assume: the actual interconnections satisfy R1; each accepted module is measured using R2 and R4; remaining junction and final-seal changes are covered by the declared envelope; service paths obey R5; material-delivery schedules satisfy every used channel capacity; and the error probability of the seed, reference, controller, or any other unmodeled shared failure is bounded by gamma.

For completion, assume either the deterministic reachability conditions of R3 hold for every module, or each unresolved module has conditional probability at least a > 0 of successful repair or replacement per paid round, uniformly over the allowed preceding histories. The second premise is a physical control assumption to be established, not a consequence of small mean defect density.

In the probabilistic case, after h rounds the probability of an incomplete or functionally uncertified object is bounded by:

$$\Pr(\text{failure}) \leq \gamma + \delta_m + R(1-a)^h.$$

Whenever the right side is at most delta, the completed object's external response satisfies the target relative tolerance with probability at least 1-delta. Its number of logical repair rounds can grow as O(log(R/delta)); inspection repetition at fixed margins also grows logarithmically. This statement does not bound physical round duration independently of size.

Proof. On the event that the shared assumptions hold and every measurement interval is valid, R2 makes each final accepted module correct. R1 then makes the assembled response correct. R5 keeps each unresolved region reachable; the separate delivery certificate ensures requested service is physically budgeted. A module's conditional chance of remaining unresolved for h rounds is at most (1-a) to the power h by repeated conditioning. A union bound over modules, measurement errors, and the shared-failure event gives the result. In the deterministic alternative, the declared inspection limit must cover R3's finite step count. R3 then supplies completion on the good-measurement event, so the last probability term is absent. QED.

The distinction between a small per-attempt false-positive rate and a bound on an eventually accepted module matters. Unlimited retries can inflate false acceptance. R4 covers the full permitted inspection history; the theorem does not silently substitute a single-test error rate.

R6 is the exact point at which this revision advances the first version. A microscopic fault fraction has been replaced by a testable response contract, a proved composition rule, a restricted constructive repair procedure, and an executable access invariant. It remains conditional on credible hardware for sensing, references, reserve actuation, and interfaces.

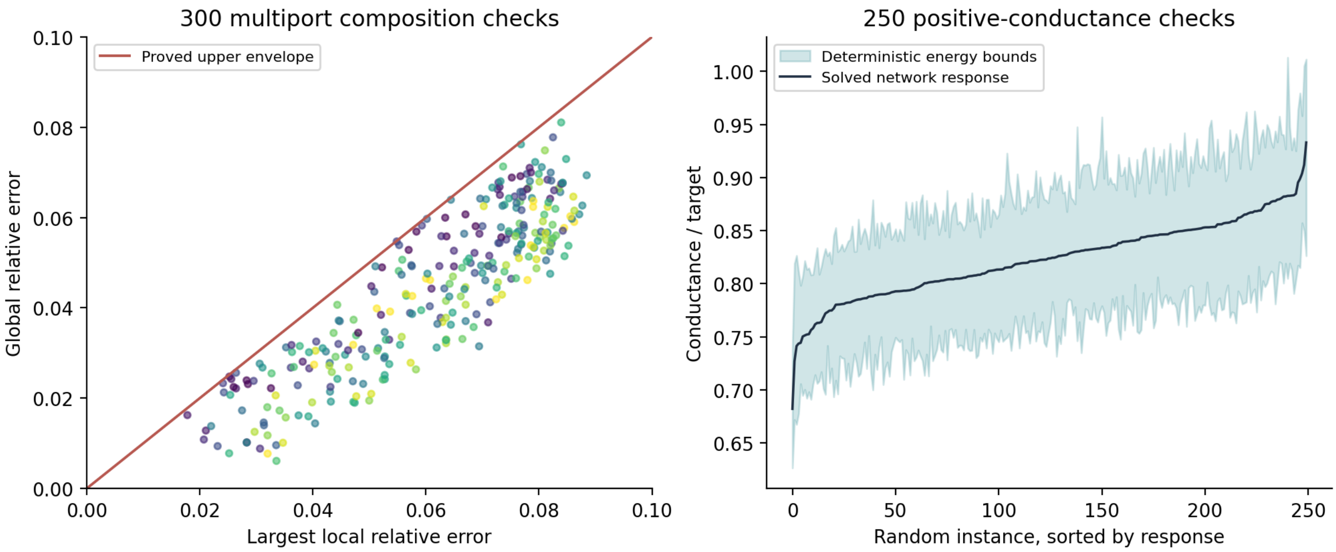

Figure 1. The composition inequality held in 300 multiport tests with correlated perturbations. The weighted-response envelope in Section 6 contained all 250 solved responses. Numerical checks expose implementation mistakes; the preceding and following proofs establish the finite statements.

5. Recoverability-complete maturation: using memory and reserve theory

5.1 What a region loses when it seals

Let r be a future-relevant functional residual in fixed, physically normalized coordinates, with finite second moment Sigma. Diagnostic information generates an information field I. Let m be the conditional mean of r given I, and let Omega be the second moment of m. Available safe local material changes have linearized endpoint map B u; their cost is lambda times squared control norm divided by two. B is fixed for the declared local comparison and must include only operations that remain physically accessible and respect protected structure. If B itself depends on the diagnostic outcome, the value is an expectation of the outcome-specific quadratic form; multiplying separate unconditional matrix averages is generally invalid. This is a local endpoint model; it does not automatically protect every intermediate chemical or mechanical state.

The imported evidence/control result from [U1, U2] gives:

The exact formula assumes unconstrained quadratic controls in the declared linear model. If a physical actuation bound is active, use the constrained optimization problem instead; the quadratic identity cannot certify that a finite depot contains enough material. R3 supplies that separate bounded-capacity guarantee for the simple module class.

$$W = BB^{\top}, \qquad R_{\lambda}(W) = W(W+\lambda I)^{-1},$$

$$J^{*} = \tfrac{1}{2}\operatorname{tr}\Sigma - \tfrac{1}{2}\operatorname{tr}[R_{\lambda}(W)\Omega].$$

Proof reconstruction. Condition on the diagnostic result. The expected squared residual separates into conditional variance plus the squared error of m-Bu. Minimizing the latter plus quadratic effort gives u = B-transpose times (BB-transpose + lambda I) inverse times m. Completing the square and averaging gives the formula. Gaussianity is unnecessary for this identity; it is needed for the particular precision formulas used below. The formula measures residual loss plus effort, not a success probability or a universally calibrated free-energy cost.

A region with no diagnostic information has Omega = 0 and no repair dividend, however much material reserve it contains. A region with no accessible actuator has W = 0 and no dividend, however well its defect is known. Orthogonal diagnostic and control subspaces also yield zero benefit.

5.2 Proposition R7: a quantitative liability for closing service

Suppose closing an inspection window or feed path reduces explained residual second moment from Omega_0 to Omega_1 and the repair Gramian from W_0 to W_1, in positive-semidefinite order. With the residual distribution held fixed, the exact increase in optimal local loss plus effort is:

$$\Delta J_{\text{close}} = \tfrac{1}{2}\operatorname{tr}[R_{\lambda}(W_0)\Omega_0 - R_{\lambda}(W_1)\Omega_1] \geq 0.$$

Proof. Inverse order implies that R_lambda is increasing in Loewner order. Expand the difference into the control decrease at fixed Omega_0 and the evidence decrease at fixed W_1. Both trace products are nonnegative. QED.

This is a fabrication application of the prior memory and reserve result, not a new quadratic-control identity. Its engineering content is a rule for the compiler: diagnostic paths, chemical access, and reference information are liabilities attached to unfinished functionality. A deletion must either discharge that functionality, replace the supporting capability, or explicitly charge the resulting loss. Shared channels are charged once as a group; pricing every dependent module as if it owned an independent channel double-counts resources.

If closure introduces a new residual, Sigma and the observation model must also change. If the accessible control map changes discontinuously, a local linear approximation may cease to apply. The deterministic R2/R3 contracts govern the positive manufacturing theorem; R7 guides resource design and does not replace those guarantees.

5.3 Complementarity and the inherited reserve threshold

For a scalar Gaussian residual, normalized diagnostic precision s and normalized repair mobility t give the net paired-service value below when their acquisition/maintenance prices are linear:

$$F(s,t) = A\frac{s}{1+s}\frac{t}{1+t} - a_s s - a_t t.$$

The Joint Reserve Law [U2] proves that a profitable nonempty pair exists exactly when:

$$A > (a_s^{1/3} + a_t^{1/3})^3.$$

At equality the zero pair and a finite pair tie. The threshold follows from Holder's inequality applied to (a_s s + a_t t)(1+1/s)(1+1/t). This exact constant belongs to the normalized scalar decision model. It is not a universal chemical manufacturability threshold. Precision is not a number of memory bits; mobility is not automatically a channel radius.

For fabrication, the implication is concrete: selecting a diagnostic site while no repair route exists, or selecting a repair route while no diagnostic can use it, can make both appear worthless. The compiler should propose them as a matched pair. The full-matrix result in [U2] further shows that protecting every one of d unrestricted residual directions costs at least d times the one-mode reserve cost. Arbitrary fine-scale future repair cannot be obtained from a constant-size reserve by changing its name.

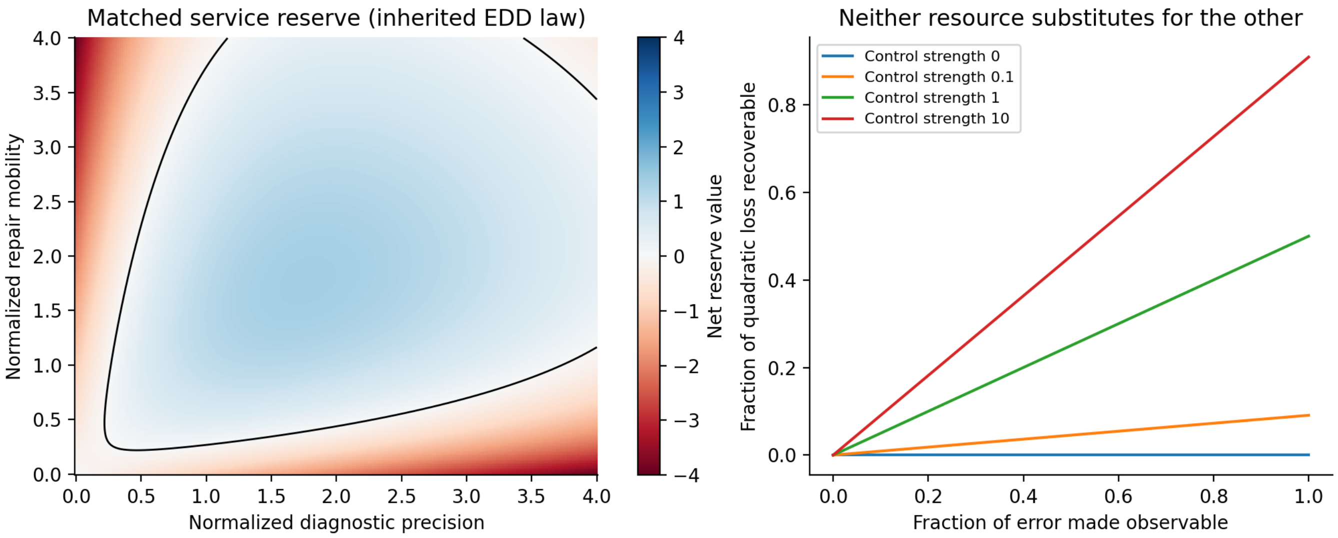

Figure 2. The plotted decision model reproduces the inherited evidence/control complementarity. Its axes are dimensionless normalized resources, not experimentally calibrated molecular measurements.

5.4 Why present-response compression is insufficient during growth

Two modules can have the same present response D but different future capabilities: one retains a depot and inspection port; the other has been sealed. They are equivalent for current static use and inequivalent for a continuation that damages and then repairs them. This is the fabrication analogue of [U3]'s requirement to define state through a declared, continuation-closed experiment grammar.

Consequently, the developmental state cannot be just D. It must also retain the finite repair grammar, reserves, reference status, service connectivity, costs, and validity horizon. Only after the relevant future grammar shrinks to final operation can interior manufacturing details be discarded without changing the promised behavior. Low predictive rank does not follow merely from a small present terminal matrix, and low rank would not by itself make planning easy.

The certificate dependencies follow [U4]'s trust-boundary discipline. An accepted record has a target/program identity, the response witness, calibration bound, material regime, remaining seal budget, service obligations, timestamp or local epoch, and verifier version. The package checks the finite numerical predicates; it is not a proof-assistant implementation or an unforgeable molecular certificate system.

6. A second route: defect participation instead of defect counting

6.1 Theorem R8: a power-weighted functional envelope

For one two-terminal experiment on a fixed connected network, let target edge conductances be g_e^0 > 0 and let V^0 be its unit-voltage solution. Define normalized target power weights and actual ratios:

$$w_e = \frac{g_e^0(\Delta V_e^0)^2}{G_0}, \qquad r_e = \frac{g_e}{g_e^0} > 0, \qquad \sum_e w_e = 1.$$

Then:

$$\left(\sum_e \frac{w_e}{r_e}\right)^{-1} \le \frac{G}{G_0} \le \sum_e w_e r_e.$$

Proof. Insert the target voltage field into the actual Dirichlet minimization to obtain the upper bound. For the lower bound, normalize the target current field to unit total current. It is still a feasible conserved flow on the same graph. Its actual dissipation is (1/G_0) times the sum of w_e/r_e. Thomson's minimum-flow-energy principle bounds actual resistance by that value. Taking reciprocals gives the lower bound. QED.

These are derived, application-specific energy bounds built from classical Dirichlet/Thomson principles [P2]. They are not claimed as new circuit theory. They provide a useful alternative when certifying every module is unnecessarily strict. A single strategically important defect can dominate the weighted sum; many unimportant defects can have little effect. Both phenomena defeat raw defect-density scoring.

6.2 Corollary R9: a restricted participation threshold

Let each edge independently be weakened from ratio one to alpha, where 0 < alpha < 1, with probability p. Let S be the weighted sum of the failed-edge indicators. To guarantee a conductance ratio of at least 1-epsilon, it suffices that:

$$S \le s_c = \frac{\varepsilon}{(1-\varepsilon)(\alpha^{-1}-1)}.$$

If p < s_c, a weighted Hoeffding bound yields:

$$\Pr(G/G_0 < 1-\varepsilon) \le \exp[-2(s_c-p)^2 N_{\text{eff}}], \qquad N_{\text{eff}} = \frac{1}{\sum_e w_e^2}.$$

Proof. R8 gives the lower response bound 1/[1+(alpha inverse minus one)S]. Solve its required inequality for S. The independent weighted indicators have mean p and range widths w_e. Apply Hoeffding's inequality. QED.

N_eff is a power-participation number for the declared experiment. It need not equal the number of components. Concentrated bottlenecks, a correlated failure of an entire cut, or alpha tending to zero destroy this favorable bound. The threshold is sufficient and conservative, not the exact percolation transition. For epsilon = 0.08 and alpha = 0.6, s_c is approximately 0.1304. At p = 0.08, a failure bound of 0.05 requires N_eff about 590. At alpha = 0.1, the same tolerance gives s_c about 0.00966. Nearly open circuits are much harder to tolerate.

This law is complementary to R6. R6 certifies every accepted response and can tolerate correlations inside those envelopes. R9 can tolerate unverified microscopic deviations but pays for independence, a nonzero surviving-conductance floor, and a favorable power distribution. Neither permits a universal error threshold depending only on the mean fault probability.

6A. Gauge-aware fabrication and an exact reserve boundary

6A.1 The new contribution and the target it actually solves

The v2 controller required a calibrated absolute conductance target for every module. That is necessary when absolute conductance is part of the promised function. It is unnecessary for a narrower but useful class: passive static devices whose specified behavior consists of voltage ratios or a terminal response up to one common positive multiplier. Multiplying all conductances by the same number changes currents, power, and usually dynamics; it leaves static Dirichlet voltage maps unchanged.

The proposed v3 contribution is a **gauge-aware reserve compiler**. It chooses a physically reachable representative of a functional equivalence class, instead of fixing an unnecessary absolute scale before growth. For scalar passive modules with bounded additive reserves, the representative-selection problem has an exact feasibility test and a minimum-material solution. A robust version includes finite diagnostic confidence, finite deposition increments, remaining seal changes, and preservation of the comparison network. An exact finite-size yield law exhibits a reserve threshold in a declared bounded-disorder model.

This is a restricted theoretical advance, not the invention of ratiometric metrology, scale invariance, interval feasibility, or graph calibration. Those ingredients have substantial prior art [P15-P17]. Independent priority of the combined manufacturing result is unverified. The new value is the explicit connection between the function quotient, reachable material intervals, statistical confidence, and the physical decision to remove manufacturing access.

The compiler must obtain permission from the *specification* to discard a scale. It cannot relax a requested current, power, timing, or absolute sensitivity specification to manufacture an easier object. A fixed external load, a contact resistance outside the certified modules, or a capacitor whose scale does not change with the conductors can break the claimed invariance. The quotient applies to all relevant conductances, including junctions unless they are ideal node identifications.

6A.2 Proposition G1: functional scale freedom and its identifiability limit

Let the complete passive network have positive scalar module conductances g_i = g_i^0 x_i. All couplings obey the named-port assumptions of R1. Define the projective response error on the grounded port space by:

$$d_{\mathrm{P}}(D, D^0) = \frac{1}{2} \ln \frac{\lambda_{\max}(D, D^0)}{\lambda_{\min}(D, D^0)}.$$

The eigenvalues are generalized eigenvalues of the two grounded responses. The quantity is unchanged if either response is multiplied by a positive scalar. For a two-terminal object it is identically zero; a nontrivial benchmark therefore needs at least three terminals or a nontrivial voltage-transfer specification. The v3 computations use four external terminals and separately score an internal voltage map.

Statement. If one common scale kappa satisfies the following local bounds, then the assembled response satisfies the same bounds and its projective error is at most tau:

$$\kappa e^{-\tau} g_i^0 \le g_i \le \kappa e^{\tau} g_i^0 \quad \Longrightarrow \quad \kappa e^{-\tau} D^0 \preccurlyeq D \preccurlyeq \kappa e^{\tau} D^0.$$

Proof. Sum the local quadratic energies and minimize over interiors exactly as in R1. The generalized eigenvalues then lie in the interval from kappa exp(-tau) to kappa exp(tau), whose ratio is exp(2 tau). QED. No factor equal to module count appears.

If D is divided by its trace, the corresponding normalized response is within exp(plus or minus 2 tau) of the normalized target in Loewner order. This does not certify relative error of a signed near-zero transfer entry. Exact common scaling preserves a Dirichlet voltage map because multiplying its harmonic equation by a nonzero scalar does not change the solution.

A useful conservative perturbation statement is available when all network edges satisfy the local envelope. Let v^0 be the target harmonic voltage with prescribed boundary voltages and let v be the actual one. In the target energy seminorm, on the zero-boundary error space:

$$\|v - v^0\|_{L^0} \le e^{\tau}(e^{\tau} - 1)\|v^0\|_{L^0}.$$

Proof. Put A = L/kappa and w = v-v^0. Harmonicity gives w-transpose A w = -w-transpose (A-L^0)v^0. The envelope bounds the left side below by exp(-tau) times the squared target norm, and the right side in magnitude by (exp(tau)-1) times the product of the two target norms. Divide if w is nonzero. QED. A pointwise voltage bound additionally requires the target's grounded evaluation norm; it is not uniform over arbitrarily ill-conditioned geometries.

No-go result for absolute calibration. Ratio observations cannot distinguish x from a common multiple of x. More generally, an experiment consisting only of ratio observations and scale-equivariant actions has the same transcript law in two worlds differing by common scale. If their absolute acceptance sets are disjoint, a decision based on that transcript cannot correctly distinguish the worlds with average probability greater than one half under equal priors. A claimed absolute certificate that accepts both is unsound in at least one world.

An absolute material increment, calibrated voltage/current standard, known time constant, or independently known constitutive parameter can break this symmetry. It then supplies real reference information and must be charged as such. The project does not claim that all physical experiments are scale-equivariant. A connected comparison graph has one scalar ambiguity; disconnected components have separate ambiguities.

6A.3 Theorem G2: exact reachable-scale interval and minimum material

Scope: proved for continuous, independently accessible, additive scalar conductance reserves. Suppose module i begins at ratio x_i > 0 and can reach any ratio in the closed interval from x_i to x_i+c_i, with c_i nonnegative. Choose a common kappa and require every final ratio to lie between kappa exp(-tau) and kappa exp(tau).

The problem is feasible if and only if:

$$\kappa_{\mathrm{lo}} = e^{-\tau} \max_i x_i \;\le\; \kappa_{\mathrm{hi}} = e^{\tau} \min_i (x_i + c_i).$$

When it is feasible, choose kappa = kappa_lo and:

$$y_i^* = \max\{x_i, e^{-\tau}\kappa_{\mathrm{lo}}\}.$$

This minimizes every positive weighted sum of added conductance, with no coupling between material prices:

$$\min \sum_i w_i (y_i - x_i), \qquad w_i > 0.$$

Proof. The reachable interval for a module intersects the admissible band exactly when x_i is at most kappa exp(tau) and x_i+c_i is at least kappa exp(-tau). Intersect these scale constraints over all modules. For a fixed feasible scale, the least admissible final ratio is max(x_i, kappa exp(-tau)). This is nondecreasing in kappa for every module, so the smallest feasible scale minimizes every stated positive linear cost. QED.

An additional admissible scale interval is included by intersecting it with this interval. However, an interval in absolute physical units requires absolute reference information. If junctions, power, or material limits couple the controls, the separable cost result no longer solves that larger problem.

For example, x = (0.72, 1.32), c_i = 0.60, and tau = 0.04 cannot meet a unit-scale 4% log-tolerance target using additions alone: the larger module already overshoots. The projective problem is feasible. Its minimum scale is about 1.26824, and the smaller module is increased to about 1.21851. Both modules then satisfy the same scale-free response contract. They do not become accurate absolute unit-conductance components.

The exact interval is an actionable compiler object. A module exposes a reachable response interval and a material price, rather than a list of desired microscopic coordinates. The compiler computes two reductions, selects the shared scale, and distributes local endpoint targets. For the declared scalar model this takes linear arithmetic work, with a reduction/broadcast depth bounded by the service graph's diameter.

6A.4 Theorem G3: finite-noise, finite-increment construction

Continuous exact actuation in G2 is an idealization. The following sufficient result has finite increments and bounded measurement error.

Use one comparison witness with unknown absolute value but stable response during the certified manufacturing window. Every x_i and every reserve capacity is expressed in the same witness-relative units after division by the nominal role value. The witness is not an accurate copy of the target material. It must still be accessible, nonzero, stable within a declared budget, and measured in the same physical regime.

At each inspection, suppose the reconstructed log ratio obeys absolute error at most e. Let the remaining seal multiply each module by a factor between exp(-beta) and exp(beta). Every repair step increases the ratio by an amount in [h_min,h_max], where h_min > 0; the total available increment is c_i. These are actuator requirements to establish experimentally, not properties inferred from a generic deposition label.

Let l_i and u_i enclose the initial true ratio. Define:

$$a = e^{-\tau + \beta + 2e}, \qquad b = e^{\tau - \beta - 2e}, \qquad \tau > \beta + 2e.$$

It is sufficient that the following interval be nonempty:

$$\max\left\{\max_i \frac{u_i}{b}, \frac{h_{\max}}{b-a}\right\} \le \kappa \le \min_i \frac{l_i + c_i - h_{\max}}{a}.$$

For each module, accept when its measured log ratio lies in:

$$\ln\kappa - (\tau - \beta) + e \;\le\; \widehat{\ln x_i} \;\le\; \ln\kappa + (\tau - \beta) - e.$$

Otherwise add one allowed increment if the reading is low. No subtractive operation is used.

Conclusion. Every module reaches acceptance in a finite number of increments, remains within its reserve capacity, and satisfies the final G1 envelope after any allowed seal change. A sufficient per-module increment bound is one plus the ceiling of the positive part of (a kappa - x_i_initial)/h_min, with an inspection after the final increment.

Proof. Initial x_i is at most b kappa. A failed low reading implies x_i < a kappa. The next increment cannot exceed b kappa because h_max is at most (b-a) kappa. Once x_i is in [a kappa,b kappa], every allowed reading passes. Until then, each step advances by at least h_min. The reserve inequality guarantees sufficient capacity to cross the lower endpoint without exhaustion. Acceptance bounds the true pre-seal ratio by kappa exp(plus or minus (tau-beta)); the seal completes the desired envelope. QED.

A high failure is excluded on the theorem's good-data event; the implementation reports it honestly if it occurs. The conditions are sufficient and conservative. They do not give a minimum-material theorem for quantized noisy repair.

For all initial ratios in a known interval [l,u], an a priori sufficient common reserve follows by using l_i >= l exp(-2e) and u_i <= u exp(2e) when initial intervals are built from an e-accurate log estimate:

$$c \ge a\max\left\{\frac{ue^{2e}}{b}, \frac{h_{\max}}{b-a}\right\} - le^{-2e} + h_{\max}.$$

For l = 0.65, u = 1.35, tau = 0.04, beta = 0.005, e = 0.006, and h_max = 0.012, this bound is approximately 0.675. The simulations allocate 1.05 units of reachable reserve per module, so the positive examples have deliberately generous capacity. Consumed material, allocated reachable capacity, and the apparatus needed to use that capacity are different costs.

The finite horizon must cover the stated increment count plus inspections. Zero-gain nucleation events violate a strictly positive h_min. A probabilistic progress model can instead use the conditional-progress version of R6, but that requires a measured progress probability and an adequate horizon.

6A.5 Theorem G4: an exact reserve-controlled yield boundary

Scope: exact reachability of the G2 local envelopes, with iid initial scalar ratios uniformly distributed on [l,u], a common additive reserve c, and no measurement, seal, or quantization error. This is not a universal chemical phase transition and not a lower bound on every possible device architecture.

Put q = exp(2 tau). Feasibility is exactly the event:

$$\max_i x_i \le q\left(\min_i x_i + c\right).$$

The critical reserve is:

$$c_* = \max\{0, ue^{-2\tau} - l\}.$$

For c >= c_*, every configuration in the support is feasible, with no independence assumption needed. For c < c_*, feasibility probability decays exponentially as the number R of modules increases. When tau > 0 and c < c_*, define:

$$s = \frac{u(1-q^{-1})+c}{u-l}, \qquad t = \frac{(q-1)l+qc}{u-l}.$$

The exact finite-size probability is:

$$P_R(c) = \frac{qs^R - t^R}{q-1}.$$

Proof. Condition on the unique minimum m. Its location can be any of R indices. All other values must lie between m and min(u,q(m+c)). Therefore:

$$P_R(c) = \frac{R}{(u-l)^R}\int_l^u [\min\{u, q(m+c)\} - m]^{R-1}\, dm.$$

Split the integral at m = u/q-c and integrate the two powers. In the subcritical range this point lies between l and u and yields the displayed formula. Here 0 <= t < s < 1, so P_R is bounded above by q s^R/(q-1). At and above the threshold the largest possible initial ratio is within q times the smallest possible final one. QED.

At tau = 0 and 0 <= c < u-l, the limiting formula is R r^(R-1) - (R-1) r^R, where r = c/(u-l). This is the familiar uniform-sample range probability. The order-statistics ingredients are classical; their reserve-fabrication interpretation and integration with G3 are the proposed contribution.

For this model only, one can define a dimensionless reserve number:

$$\mathcal{M}_{\mathrm{reserve}} = \frac{e^{2\tau}(l+c)}{u}.$$

Its boundary at one exactly separates support-wide G2 reachability from asymptotically vanishing iid yield. Adding confidence, finite increments, and seal margins moves the sufficient engineering boundary upward according to G3. There is no evidence for a material-independent universal fabrication number.

For l = 0.65, u = 1.35, and tau = 0.04, c_* = 0.596207. At c = 0.55 the exact yields for R = 16, 64, and 256 are about 0.69824, 0.06042, and 0.000000265. At c = 0.60 they are all one in this ideal model. These numbers come from the formula, not a fitted transition curve.

Unbounded-tail limitation. If iid initial ratios have unbounded upper support and a finite lower endpoint, then a fixed finite additive reserve cannot maintain these local projective contracts as R tends to infinity. The maximum diverges while the minimum plus reserve remains bounded in probability. This invalidates a tempting claim that scale freedom alone solves arbitrary manufacturing disorder. Culling, replacement, larger reserves, a different contract, or a genuinely bounded process distribution is necessary. A failure of these sufficient local contracts need not imply failure of a particular global scalar function.

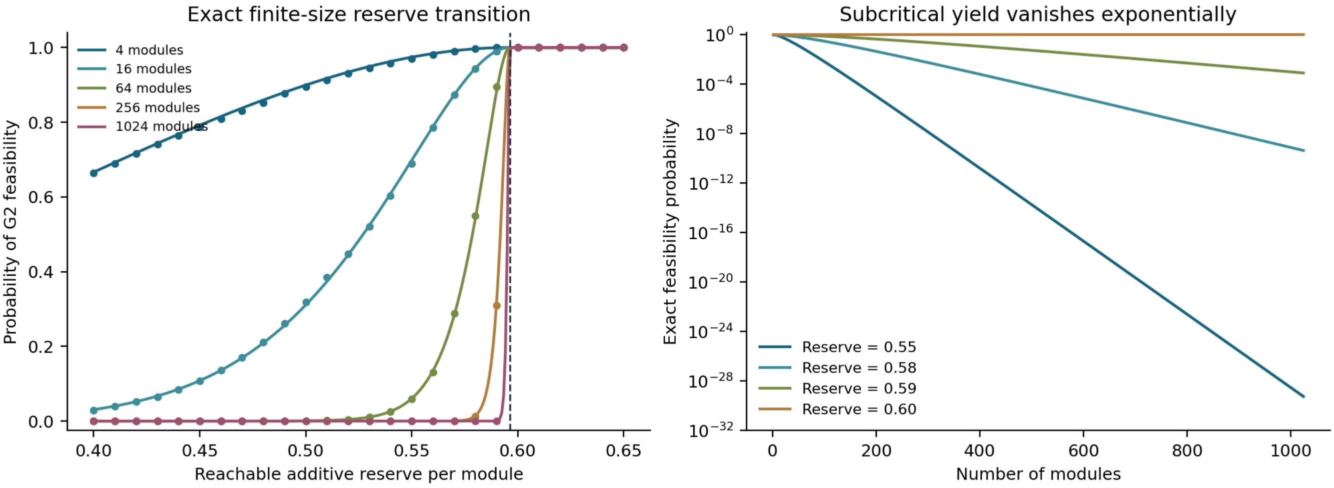

Figure 3. Exact G4 curves and independent-array Monte Carlo checks. For each size, the same 5,000 arrays are reused across 31 reserve values. Finite increments and measurement costs belong to the separate G3 manufacturing experiments.

6A.6 Relative metrology: what it removes, and what it cannot remove

Let z_i = ln(x_i). A paired comparison of neighboring modules uses the same positive detector gain for both readings and divides out their known nominal role ratio. With additive offsets removed and both readings taken in a stable regime, the log ratio cancels that shared gain exactly. An unknown common material multiplier cancels as well when the witness and actuator units scale consistently.

This is ordinary ratiometric reasoning, not a new metrology principle [P17]. It does not cancel different gains on the two arms, additive offsets, contact errors, nonlinearity, or temporal drift between readings. Averaging logarithms of ordinary noisy measurements is not automatically unbiased; the log-error model must be validated rather than inferred from an ADC specification.

Represent the temporary comparison graph by an oriented incidence matrix B. Fix one numerical reference coordinate to zero; this is a gauge convention, not an absolute material calibration. With B_g denoting the matrix with that column deleted:

$$y = B_g z + \varepsilon, \qquad \hat{z} = (B_g^\top B_g)^{-1} B_g^\top y.$$

Proposition G5, established calibration mathematics applied here. If the edge-average error is conditionally centered with joint sub-Gaussian proxy (sigma squared/n) times the identity, the error of coordinate i has proxy (sigma squared/n) rho_i, where rho_i is diagonal entry i of the grounded graph-Laplacian inverse. For independent Gaussian edge errors this is the exact variance. The rho_i are effective resistances to the reference in a unit-resistance comparison graph [P15].

Proof reconstruction. The estimator error is a fixed linear transformation A epsilon. Its covariance proxy is (sigma squared/n) A A-transpose. Matrix multiplication gives A A-transpose = (B_g-transpose B_g)^(-1). Apply the scalar sub-Gaussian tail bound to each row. QED.

For at most H inspections of R nonreference modules, a simultaneous log-error radius is:

$$e_{\text{stat}} = \sigma \sqrt{\frac{2\rho_{\max}}{n} \ln \frac{2RH}{\delta_m}}.$$

The graph and the noise proxy must remain valid throughout the declared inspection window. Fresh conditional noise bounds cover adaptive repair decisions. Arbitrary componentwise bounded variance or arbitrary correlated bias is insufficient. Numerical inference error, drift, and other bounded errors must be added to this radius; they are not averaged away.

The effective-resistance identity and its dimension dependence are prior art [P15]. For finite nearest-neighbor boxes of side n, worst reference variance scales as order n in one dimension, log n in two, and a bounded constant in three. A short finite-box argument uses cosine eigenmodes of the free-boundary grid: their squared amplitudes are bounded by a constant times n^(-d), their nonzero eigenvalues below by a constant times the squared mode index divided by n squared, and the resulting shell sum is respectively bounded, logarithmic, or linear before the prefactor n^(2-d). Matching lower bounds follow from disjoint unit-current cutsets; a corner cut alone provides the three-dimensional constant [P2, P15].

Thus fixed confidence over all modules needs order log R samples per edge in a regular three-dimensional comparison network, rather than a constant sample count. Thin bottlenecks, a long reference stem, or a tree can destroy that advantage. A solid three-dimensional object is not sufficient if its comparison graph is effectively one-dimensional.

Differential-bias no-go. Write a systematic comparison error as a gradient B_g v plus a cycle component c with B_g-transpose c = 0. Least squares assigns the gradient to the material state and leaves only the cycle component in its residual. In particular, y = B_g(z+v) has a perfect cycle-consistency certificate while the inferred material state is wrong by v.

This is an exact counterexample to the idea that redundant loops can validate their own standards. It is consistent with classical blind-calibration ambiguities [P16]. The v3 simulations deliberately retain this failure. A bound on differential bias requires an additional physical model, independently checked comparison reversals, another measurement modality, or external reference information. No number of repeats of the same biased measurement closes this gap.

6A.7 Local computation and the latency that calibration adds

The simulator uses a factored finite linear solve to evaluate the estimator efficiently. It does not pretend that this factorization is an autonomous molecular operation. A separate implemented neighbor-message algorithm solves the same problem:

```
initialize one scalar z_i = 0 at each comparison node
repeat:
    r_i = sum of oriented measured differences at node i
          minus sum over neighbors of (z_i - z_j)
    z_i = z_i + omega * r_i
    reduce maximum residual over the retained service tree
until the numerical-error certificate is small enough
broadcast the witness value and subtract it at every node
```

Choose omega = 1/(maximum degree + 1). The mean stays zero mathematically, and all nonconstant modes contract. The final reference subtraction is a broadcast, not a local atomic operation. For N comparison nodes and graph diameter d_C, a conservative graph-gap bound is 2/((N-1)d_C).

To verify that bound, sum the squared difference between each pair of nodes and bound each by its path length times total edge energy. Since the sum of pairwise squared differences is N times the zero-mean squared norm, the stated Poincare bound follows. If r is the residual, the numerical error of any reference-relative coordinate is therefore bounded by:

$$e_{\mathrm{num}} \le \frac{\sqrt{2N}}{\lambda_{\mathrm{lower}}} \|r\|_\infty .$$

This bound is conservative but needs no centrally stored eigenvector. Each node stores only local estimates, neighbor information, and the counters/budgets used by the reduction. The implementation verified this local solver on 16, 64, and 216 nodes. It required 119, 190, and 441 synchronous update rounds for a certified numerical radius of 0.00001. Actual errors were smaller. These are algorithmic rounds, not measured seconds.

On regular boxes, diffusion-like iteration takes order n squared times a logarithmic precision factor. A small estimation variance in three dimensions does not imply rapid local convergence. A solver that pins a single reference during every update can have an even slower collective mode; the implemented solver instead preserves zero mean and fixes the numerical gauge afterward.

Paired probes sharing a module cannot generally run simultaneously. The code colors comparison edges into disjoint matchings and charges each color slot, its sample count, and repeated inspections. Molecular electronics, communication energy, parallel comparator count, ADC bandwidth, isolation, and controller fabrication remain apparatus costs. A hierarchical or analog implementation might reduce latency, but no unbuilt fast solver is used to claim an achieved fabrication time.

6A.8 Theorem G6: fabrication with one uncalibrated witness

Status: a proved conditional synthesis; candidate v3 contribution, priority unverified. Consider the scalar passive module class of G1. Assume:

1. The specification explicitly permits one common conductance multiplier.

2. Nominal roles, geometry, contacts, and external loading satisfy the declared passive quotient model.

3. A connected comparison network provides the finite-confidence G5 estimates, including any numerical and systematic-error margins.

4. A witness with unknown absolute value is stable within the accounted budget; all capacities and increments use its consistent relative units.

5. The compiler finds a G3 feasible scale, and material reserves, service throughput, and inspection horizon satisfy G3.

6. Both material access and comparison dependencies remain available until all affected modules are certified; remaining seal changes stay within beta.

Then on the simultaneous good-data event, every module completes finite repair and the final object's projective response error is at most tau. If the joint probability of shared-assumption failure is at most gamma and the statistical budget is delta_m, failure probability is at most gamma + delta_m on a domain where G3 feasibility and the deterministic resource conditions are assured.

For a random domain where robust feasibility itself can fail, a valid statement is that success probability is at least the probability of feasible, valid shared conditions minus delta_m. One must not silently replace that feasibility probability with one. G4 describes a simpler exact model; it is not the measured yield law of noisy G6 hardware.

Proof. G5 and the numerical/systematic margins give simultaneous valid inspections. G3 gives finite reachability and the final common-scale envelope while the access invariant preserves the required operations. G1 composes the local envelopes without a module-count error factor. A union bound charges the stated shared and statistical failures. QED.

The witness can be an imperfect conductor; its absolute value is absorbed into the allowed common scale. This removes the need for an accurate absolute target standard at each module. It does not remove target-program integrity, paired-ratio fidelity, witness stability, or independent assurance of differential bias.

6A.9 A new closure obligation and a falsifiable physical proposal

The material-supply tree and the metrology graph carry different dependencies. A region may have enough material while its state remains inferable only through a comparison path crossing another region. The earlier postorder material rule alone does not certify this dependency.

The conservative implemented rule retains the complete comparison backbone until every module has its final pre-seal certificate. It then releases the backbone and executes the ordinary local postorder seal. Certificates remain valid during the intervening wait only under the declared response-stability budget. Waiting indefinitely is not covered.

The operating and promised maintenance grammar must both respect the allowed scale freedom. If a later action needs absolute current, energy, or a calibrated material increment, the object must retain or reacquire that reference information. The continuation-equivalence principle from [U3] prevents present-response compression from silently deleting a future requirement.

Earlier removal may be possible by recomputing a certified remaining comparison graph, by retaining a valid reference-transfer witness, or by eliminating a node with its sufficient statistic and covariance. Such elimination can create dense virtual couplings. Constant-port functional compression does not imply constant-memory metrological elimination for arbitrary three-dimensional graphs. That optimization is left open.

The minimal physical test is a four-module resistive bridge with conductor/dielectric separation, nonidentical nominal roles, incremental parallel reserve paths, and a retained pair-comparison channel. First test the controller with switchable passive resistor reserves. That validates the control mathematics, not developmental chemistry. Then replace the reserve actuator with a measured, scaffold-compatible deposition process and repeat the same test after material conversion.

Use three independent grounded voltage patterns to characterize the four-port response, and also test the prescribed high-impedance voltage output. Vary shared detector gain and a common material scale, then inject a differential comparison bias as a negative control. Cross an independently measured reserve boundary. Compare against a fixed representative and against an equally capable conventional ratio controller. The latter is expected to tie.

Support for the physical claim requires final function after conversion, repeatable bounded increments, retained comparison access, quantified differential bias, and a measured material ledger. Failure to obtain a bounded increment or a stable paired-ratio measurement falsifies the proposed backend even if a software demonstration passes. A favorable bridge voltage alone does not establish the full response contract or a general nanofabricator.

7. Developmental compression, seed information, and honest leverage

7.1 A resource-bounded definition

Fix a declared reusable platform H: interpreter, species design, chemical repertoire, apparatus geometry, calibration procedure, and physical law model. Let G be the target genome, S its seed initialization, E the target-dependent environmental program, and U any target-dependent intervention transcript. Define developmental complexity at geometry/function tolerance epsilon, failure probability delta, and resource budget B by:

$$K_{\mathrm{dev}}^{\varepsilon,\delta,B}(X \mid H) = \min\{L(G) + L(S \mid G) + L(E) + L(U)\}.$$

The minimum ranges only over executions meeting the declared resource budget and acceptance probability. A specialized feedstock recipe, lithographic mask, hidden prepattern, calibrated target table, or separately designed building-block library must be charged to H if reused across the declared target class, or to the target-specific description otherwise. Reusing H across n_jobs jobs permits an explicit amortized charge L(H)/n_jobs; calling H universal does not make it zero-cost hardware.

7.2 Theorem A: compressibility and its obstruction

If a fixed computable grammar P generates a family X_n and its physical backend meets the declared finite resources, the target-dependent description has length at most L(P) plus a self-delimiting description of n, hence O(log n). For a d-dimensional family with N proportional to n to the power d, this is O(log N). The condition on the backend is essential: a short nonterminating search is not a fabrication method.

Proof. Encode the fixed generator once and its finite size parameter. Execute the generator through the assumed backend. QED.

The converse follows by counting. For N independent q-ary target labels, most targets require order N log_2 q bits. At Hamming tolerance k, one description covers at most the size of a q-ary Hamming ball in the deterministic case. Thus a covering set requires at least q to the power N divided by that ball size descriptions. The v1 package gives the analogous probabilistic counting formulation. Random exact microtextures and arbitrary unique wiring therefore remain expensive. Functional equivalence can enlarge acceptable sets, but it does not erase information that the requested target genuinely requires.

For exact deterministic computable execution, ordinary conditional algorithmic complexity obeys K(X given H) no greater than the developmental description plus a fixed interpreter constant. Resource constraints can make developmental complexity larger. For approximate stochastic construction, compare tolerance classes or a separated target packing instead of claiming that the exact final atomic microstate was fully specified by the seed.

A terminal response of k ports has at most k(k-1)/2 independent real coefficients in the passive grounded class. Over a bounded, well-conditioned response family, its finite-resolution description may scale as that dimension times log(1/epsilon), independently of interior atom count. The geometry and all other protected functions must still be encoded. This is a reduction of the specification's relevant degrees of freedom, not amplification of algorithmic information beyond the program and its inputs.

7.3 Theorem E: positional information and a boundary-complexity warning

If a local decision must distinguish R equiprobable developmental regions with error probability e, Fano's inequality requires at least log_2 R minus the binary entropy of e minus e log_2(R-1) bits of mutual information in its available observations and state. A lineage word of length O(log R) can meet the corresponding address-size order. A single scalar gradient with fixed noise cannot supply unbounded address precision.

The executable grid family inherits local integer counters from a neighbor and applies a fixed parity grammar. Counters require O(log N) bits per region; their total temporary physical storage can be O(N log N). This is compatible with a logarithmic seed description, but is not negligible molecular machinery. Coordinate copying, orientational coherence, and the interpreter are ideal in the supplied simulations. Independent anchor checks and error-correcting fields are engineering proposals, not completed chemical implementations.

Bounded ports are a real restriction. If a three-dimensional module exposes all surface features, k can grow as its volume to the power 2/3. A dense k-by-k response certificate can then grow faster than its interior volume. Full-field optical or elastic objects do not automatically gain the bounded-port compression advantage. Lumped electrical, fluidic, or selected mechanical components with a few controlled interfaces are the plausible first targets.

7.4 Morphogenetic leverage, autonomy, and compilation ratio

Use B_epsilon(X) for the number of bits in a fixed explicit target code at the declared tolerance; do not use an undefined count of continuous physical degrees of freedom. Let I_paid be the developmental description plus target-specific apparatus/feedstock information and a declared platform amortization. An auditable control-leverage ratio is B_epsilon(X)/I_paid, reported alongside total physical memory, work, yield, and precision. This ratio measures savings relative to an explicit code. It is not a Shannon-information creation ratio and is not invariant to a change of target coding convention.

The physical compilation ratio should use the same paid denominator and a declared finite-resolution output alphabet. Reporting it separately with an inflated atomic-degree numerator would double-count the same conceptual advantage. For functional targets, packing or covering entropy of the allowed response class is a more principled numerator than atom count.

Fabrication autonomy requires several measurements: target-specific bits supplied after seeding, externally selected intervention episodes, fraction of corrective decisions made locally, dependence on target-independent pumping and global chemical stages, and communication latency. A seed-only target channel can be highly informationally autonomous while depending on an external pump. The new simulation is autonomous under its fixed program after seeding; its substrate, references, channel capacities, and scheduling abstraction are assumed apparatus. The proposed first wet experiment has lower autonomy and must report its external feedback explicitly.

7.5 Fabrication as a noisy physical channel

Let W select one target from a finite declared family; the seed and all target-specific preparation encode W, and noisy dynamics produce X'. The success test must distinguish the selected target to the stated tolerance. Fano's inequality bounds the required mutual information about W in the output, while data processing prevents independent thermal noise from creating more information about W than the charged inputs carried. Copying one selected motif many times gives high physical throughput, not many newly selectable target bits.

A fabrication capacity region is the set of simultaneously achievable target-family size, tolerance, error probability, time, energy, feedstock mass, apparatus size, and explicit control length. Reliable selection bits per second and physical units instantiated per second are different rates. The familiar binary-symmetric-channel capacity 1-h_2(p) is only an ideal communication comparison; no material decoder achieves it merely because assembly is described as a channel. The useful concrete capacity statement here is R6's restricted tradeoff between functional modules, inspection confidence, reachable repair, and paid completion time.

8. Finite grammar, network universality, and compilation

8.1 Theorem B/F: a restricted finite fabrication basis

Status: conditional constructive theorem, not a demonstrated molecular universal constructor. Assume active finite-state macrocells can read and copy finite binary tapes, grow oriented nearest-neighbor scaffolds, create insulated routed connections and unit positive resistors, perform the bounded sensing/repair primitives, and preserve their material contracts. Then any finite positive rational resistor network has a finite developmental description executable by this basis. Any finite positive real network can be approximated to a prescribed response tolerance when sufficient geometric, conductance, and resource range is permitted.

Proof sketch. A positive rational conductance p/q times the unit value is realized by p parallel chains of q unit resistors. A finite netlist can be interpreted by a fixed machine. In three dimensions, finitely many bounded-degree paths can be routed using finite subdivision and separated crossings. Positive finite conductances give continuous finite terminal response under sufficiently small perturbations. Apply the maturation contracts to realizable submodules and junctions. The number of primitive operation types need not grow with netlist length; tape, component count, routing volume, and runtime generally do. QED under the stated primitives.

This result says nothing comparable for arbitrary semiconductors, nonlinear electronics, quantum devices, superconductors, catalysts, or arbitrary mechanical machines. Rational approximation through many unit elements may be very inefficient. Passive, static tiles do not automatically implement active tape machinery. Algorithmic self-assembly and intrinsic universality already establish powerful related formal constructions [P8, P9]; the physically unbuilt substrate remains the limiting assumption here.

An ingredient alphabet and a species alphabet are different. Four nucleotide monomers do not mean four independently addressable molecular species: polymers with different sequences are different chemical objects, and their copying and processing machinery must be counted. The new code has a bounded set of output roles and primitives; it deliberately reports the number of chemically realized species as unknown.

8.2 Growth Genome Intermediate Representation

A practical genome has five linked layers: a geometry grammar, material-compatible module templates, port-response targets, a service graph, and guarded maturation rules. Its intermediate representation must preserve dependencies across these layers. A schematic record is:

```
{
  "version": 2,
  "extent": 8,
  "dimension": 2,
  "motif": "parity_conductance",
  "ports": 2,
  "eta": 0.08,
  "seal_bound": 0.01,
  "reserve_ratio": 0.9
}
```

This capsule is executable with `contract_genome.py` and the declared simulator configuration. The fixed interpreter expands the nonperiodic Thue-Morse parity family, assigns bounded conductance roles by inherited counters and edge orientation, and generates a nearest-neighbor service tree. The capsule is not the full cost of a general language or compiler. Its inspection confidence, actuation increments, hardware calibration, and transport capacities are charged runtime/configuration inputs. The original v1 midpoint-split and motif compiler is retained for irregular 2-D and 3-D geometry.

Each canonical demo capsule is 126 bytes, or 1,008 bits; the grammar interpreter source is about 3 kB, excluding dependencies and hardware. A packed three-bit role list for 300 fixed module positions is only 900 bits, so these tiny prototypes do not themselves demonstrate net description compression. The proved advantage is asymptotic for the size-varying family under a shared, paid interpreter. Uncompressed storage of those 1,008 bits at two ideal information bits per DNA base pair would require at least 504 base pairs. A shorter semantic encoding changes the code and its charged decoder. Addressing, coding redundancy, state transitions, and the physical interpreter are additional and are not chemically compiled here.

The local transition sequence is grow, provisionally differentiate, perform material conversion while service remains open, inspect, add an allowed reserve increment or reject, certify, await child acknowledgements, and seal with a final-damage margin. Molecular steps may require a different ordering for incompatible chemistries. Any reordered plan must revalidate its witnesses.

8.3 A practical compiler

```
compile(target, platform, tolerance, risk, resources):
    define geometry, interfaces, functions, and operating regime
    reject element balances or process temperatures outside platform
    search repeated motifs and hierarchical geometry descriptions
    partition into bounded-port modules where the function permits
    choose realizable material templates, including junction templates
    allocate response margins, measurement confidence, and seal drift
    propose diagnostic and repair-access resources as matched bundles
    construct a capacity-feasible service graph and growth schedule
    prove local reachability for simple modules; bound or flag others
    attach response witnesses and closure dependencies
    lower supported primitives to the chosen physical backend
    simulate held-out faults, common-mode failures, and final conversion
    emit genome, physical bill of materials, certificates, and limitations
```

Only the bounded grid family and the earlier geometry compiler are implemented. A general multimaterial inverse compiler is an open problem. The algorithm must never emit an unsupported local primitive as though lowering it to chemistry were complete.

The optimization objective includes failure probability, time, free-energy/material cost, number and cross-talk of species, genome complexity, inspection effort, and specialized apparatus. Full shortest-program minimization is uncomputable. Even finite recipe selection includes Set Cover as a special case: targets are requirements and a recipe satisfies a subset at a cost. That restricted compiler is NP-hard. Geometry, scheduling, and nonlinear chemistry add difficulties; the finite special-case hardness is enough to reject an assumed universally easy compiler.

Useful approximations include grammar induction over known motifs, bounded-depth constructive solid geometry, typed graph rewriting, mixed-integer scheduling of module templates, and a differentiable physical surrogate inside an explicit validity region. Learned local rules should be tested against adversarial continuation states and calibration shifts. A neural rule's performance on a finite target set is not a universality or reliability proof.

8.4 The v3 gauge-aware compiler pass

Before material allocation, the compiler checks whether the declared function is invariant under a positive common conductance multiplier. If absolute current, power, delay, finite external loading, or an unscaled junction matters, it retains the absolute R6 contract or expands the specification; it does not discard those requirements.

For the quotient-compatible class it adds the following instructions to the inherited growth grammar: provision a stable comparison witness; create bounded-degree local pair-comparison links; reserve capacity and guard bands; reconstruct relative log responses with a finite confidence budget; reduce the feasible-scale interval; select its lower endpoint; execute bounded incremental repairs; retain both material and comparison access; issue a common-epoch completion acknowledgement; seal with the declared margin.

A permitted gauge removes one global scalar requirement, not the R-1 independently specifiable relative degrees of freedom of a generic R-module network. Sublinear seed descriptions still come from the target family's generative structure. Runtime diagnostic state and O(R) generic hardware do not disappear.

The module comparisons are the line graph of the physical junction graph: modules sharing a junction can be compared through local switches. An additional short link connects one module to the stable witness. The target family and all comparison links are generated by the fixed interpreter. The seed does not contain the dense covariance matrix used for offline numerical evaluation. A uniform radius bound and operating budgets are charged as part of the compiler/environment specification.

Each supplied v3 capsule occupies 384 UTF-8 bytes including its final newline. This is 3,072 stored bits before molecular encoding, error correction, or the shared interpreter. The small demonstrations do not show net program-size compression over packed role labels. The asymptotic compression claim remains restricted to the fixed generative family and charges the interpreter and apparatus.

The scalar G2 optimization is exact linear-time arithmetic. G3 is a conservative feasibility pass. It does not make general developmental compilation easy, supply an autonomous general CAD compiler, or solve the chemistry of the primitives. The emitted v3 JSON capsules record the allowed functional quotient explicitly; a quotient must never be inferred merely because it increases simulated yield.

For linear elastic or hydraulic analogues, the same scale idea can apply to a suitably declared static response with prescribed boundary data. It transfers only if the actual constitutive law, couplings, and actuator reachability preserve the assumed positive quadratic form. Arbitrary materials, nonlinear motion, and dynamic devices do not follow.

9. Error correction beyond the new contract theorem

The original exact-object obstruction remains. If n independent final defects are each fatal and each occurs with probability at least u, perfect yield is at most (1-u) to the power n, hence at most exp(-nu). Proofreading before an irreversible operation cannot correct faults introduced after its last effective diagnostic and actuator. The new architecture addresses this by testing after material conversion, retaining a bounded repair path, and explicitly reserving a final-seal margin. It does not repeal the obstruction for unbounded late failures.

The v1 functional redundancy theorem also remains valid within its scope. For R modules each tolerating any fewer than rho b faulty subcomponents, independent final subcomponent error p < rho gives the Chernoff union bound:

$$\Pr(\text{failure}) \leq R\exp[-bD_{\mathrm{B}}(\rho\|p)].$$

A sufficient redundancy is log(R/delta) divided by that binary divergence. A local-stochastic bound on probabilities of all specified fault subsets gives a weaker sufficient threshold, of the form p < rho/e. Low marginal fault density alone supplies neither bound. These are standard concentration/coding ingredients; a real physical error-correcting grammar must establish their hypotheses and the device's fault-tolerance contract.

For active maintenance, define a correctable defect set by actual reachable repair actions, a repair radius by the accessible service neighborhood, latency by sensing plus transport plus chemistry, redundancy by extra geometry/state/material, and catastrophic failure by loss of the functional contract or all safe repair routes. A defect density can be low and catastrophic if it lies on a critical cut or in a shared seed reference. Correlated damage and reference corruption need explicit separate budgets.

No universal scalar error threshold has been established here. There are several independent limiting margins: diagnostic identifiability, repair reachability, transport capacity, available time, material compatibility, and shared-reference reliability. A minimum of normalized margins can be an engineering screening number, but naming it a Morphogenetic Fabrication Number would not establish a physical phase transition.

The source EDD reserve model does possess a sharp onset for a profitable matched pair. R9 supplies a restricted concentration threshold. The v1 redundancy-access reversal supplies another finite optimum. These are different phenomena and should not be collapsed into one claimed universal manufacturability constant.

10. Transport, concurrency, occlusion, and energy

10.1 Why extra redundancy can worsen reliability

The v1 slab model maintained concentration c_0 at both faces a distance ell from the center, with diffusion constant D and volumetric consumption r_0. Its stationary minimum was:

$$c_{\min} = c_0 - \frac{r_0 \ell^2}{2D}.$$

With effective repair rate proportional to concentration, increasing redundant volume while allowing ell to grow can lower repair faster than redundancy helps. For ell = a_g b to the power 1/d, the model gives a repair rate proportional to the positive part of 1-kappa b to the power 2/d. The resulting Chernoff exponent has a finite interior maximum under the specified fault/conversion model. This is the v1 redundancy-access reversal; it limits that model's reliability certificate, not all architectures.

The proposed repair is to constrain the largest distance to a maintained supply route and to keep that route open until dependent functions mature. R5 prevents logical occlusion; concentration or capacity calculations prevent a merely connected but starved network.

10.2 Material transport equations and bounds

For reagent j, a model with advection is:

$$\partial_t c_j + \nabla \cdot (c_j \mathbf{u}) = D_j \nabla^2 c_j - R_j + S_j.$$

Pure diffusion has characteristic time L squared/D. In a slab with steady volumetric use, the dimensionless depletion r_0 ell squared/(D c_0) must remain below the geometry-dependent positivity bound. Maintaining c_0 requires actual reservoirs and a flux budget. Diffusion alone does not repeatedly refill an arbitrary sealed interior.

For a cylindrical laminar service channel of radius r, length ell, viscosity mu, and pressure drop Delta P, the continuum Poiseuille estimate is:

$$Q = \frac{\pi r^4 \Delta P}{8 \mu \ell}, \qquad P_{\text{pump}} = Q \Delta P.$$

This formula assumes a continuum Newtonian fluid and suitable boundary conditions; it is not asserted valid in molecular-width channels. For water-like viscosity 0.001 Pa s, a 10-micrometer radius, 1-cm-long channel at 100 kPa gives about 3.9e-11 cubic meters per second, or 2.35 microliters per minute. A 1-micrometer radius at the same length and pressure gives 10,000 times less flow. Narrow channels cannot be made adequate merely by adding a pump label.

A distributed service tree can allocate larger upstream channels. Its radii, pressure drop, fluid volume, heat, structural weakening, and eventual removal are part of the object/apparatus budget. Under an ideal equal-pressure/laminar design, distributing flow with radius roughly proportional to the cube root of branch flow is one familiar optimization pattern, not a guarantee for reactive nanoscale transport. The v2 delivery model instead declares finite edge capacities and checks every batch against them; it does not solve a hydraulic inverse design.

10.3 Theorem D: physical parallel-growth limits

At bounded density and finite signal/growth speed v from a compact seed, occupied volume lies inside a causal region of diameter proportional to vt. In dimension d, the number of separated finite-size units is at most a constant times (vt/a) to the power d. Sustained exponential growth of dense matter from one seed is impossible at fixed local speed; early branching can only remain exponential before spatial crowding or transport limits bind.

For target volume V, material density rho_m, and inlet mass rate F, fabrication time is at least rho_m V/F. A surface front with bounded normal speed requires time of order L/v for a compact object. Diffusive supply from an exterior boundary can impose an L-squared time scale. Distributed deposition inside a perfused porous scaffold can remove that interior diffusion distance, but cannot evade construction of the scaffold, the inlet flux bound, or heat removal. It provides an asymptotic advantage only under an explicit scaling of internal access and boundary supply.

In R6, logarithmic logical retry rounds can coexist with fabrication time that grows linearly or worse with size. For example, R = one million, conditional success a = 0.6, and completion risk 0.01 require 21 rounds. Twenty-one slow, transport-starved rounds do not imply a fast factory.

10.4 The simulator's explicit transport schedule

The v2 network grows in local depth layers from a corner seed. Each proposed layer reserves its scaffold and functional-material demand. The service tree's edge capacity equals the root rate multiplied by its descendant-node fraction; these capacities are assumed engineered resources, not the capacities of identical microscopic tubes. Demand is summed upstream. A batch duration is at least the maximum, over every edge and the root, of demand divided by its capacity, plus the longest signal-path delay. Each local chemical action also takes a positive minimum time.

This gives a conservative, executable reservation schedule with a mass ledger. It is substantially less detailed than a reaction-diffusion or hydraulic model and can be inefficient for an unbalanced moving front. There is no uncharged interior reservoir plane or instantaneous supply to a sealed descendant. The model does assume nonblocking routing, validated channel capacities, and local storage for batch delivery. Its output time is in abstract units and is not converted to seconds.

10.5 Thermodynamics and the price of reliability

Growth and repair consume chemical free energy and export entropy. Local reversible elementary steps must satisfy the applicable detailed-balance or local-detailed-balance constraints. Driven proofreading requires maintained chemical potential differences; a unidirectional transition in code is not thermodynamic evidence.

At 300 K, k_B T is about 4.14e-21 J. A simple equilibrium discrimination ratio p relative to a favored state needs a free-energy separation of order k_B T log(1/p), about 13.8 k_B T for p = 1e-6. This is a two-state equilibrium estimate, not a universal minimal dissipation for arbitrary repair. Fuel-driven repeated tests, kinetics, degeneracy, binding barriers, and time constraints change the cost. Landauer's k_B T ln 2 bound applies to logically irreversible erasure under its assumptions, not to every act of copying an instruction into matter.

At 10 k_B T per turnover, one billion control turnovers would be about 4.1e-11 J, whereas 1e20 turnovers would be about 4.1 J. These arithmetic figures do not price synthesis, reservoirs, pumping, cooling, reagent manufacture, or irreversible material conversion, which may dominate. The new code reports material and inspection counts; it deliberately does not report an uncalibrated energy number as if it were measured free energy.

For a locally detailed-balanced reaction network with forward and reverse event fluxes J_r^+ and J_r^-, the entropy-production rate has the familiar nonnegative form k_B times the sum of (J_r^+ - J_r^-) log(J_r^+/J_r^-). Chemical potentials and temperature specify the free-energy drive.

Incorrect bonds can be kinetically rejected without making every process equilibrium-limited, but maintaining that kinetic cycle consumes fuel and produces waste. A credible chemical backend must specify the reactions and their reservoirs.

Heat can dominate controller erasure. As an illustrative continuation of the v1 budget, 0.02 mol of material conversion at an assumed 100 kJ/mol releases 2 kJ. In 25 minutes this is 1.33 W inside a cubic centimeter. A uniformly heated 1-cm slab with thermal conductivity 0.6 W/(m K) and fixed-temperature faces would have a central temperature rise of about 28 K. These are assumed values, not measured properties of a selected chemistry; they demonstrate why a wet informational scaffold may need staged or externally cooled conversion.

A reaction step on every atom is unavoidable as chemistry, but need not be an individually addressed instruction or serial operation. The architecture seeks small explicit atomic-control fraction by recruiting prevalidated molecules, particles, doped components, and bulk conversion chemistries. Unknown atomic interfaces cannot be repaired by declaring that fraction small. Define f_atomic as the number of atoms whose individual placement/state must be explicitly specified for this target divided by total atoms. Using a prevalidated functional nanoparticle charges its internal manufacturing process to the component platform rather than supplying new per-atom placement instructions for every object. A small f_atomic reduces target-specific atomic control, not the number of atoms that chemistry must process or the cost of producing those components.

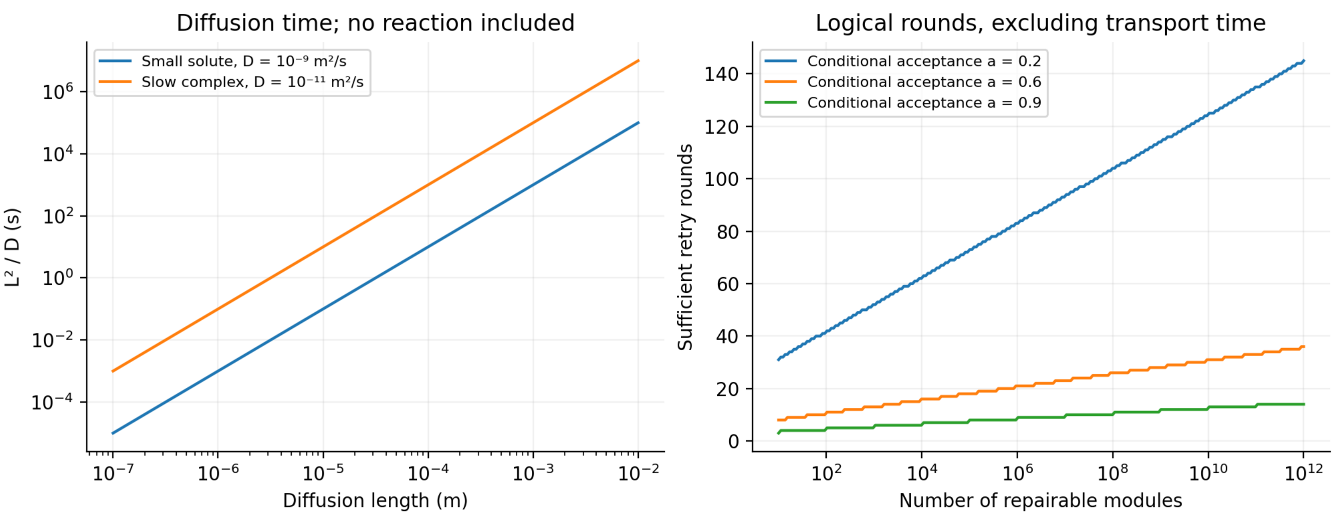

Figure 4. Diffusion time and retry-round count describe different bottlenecks. The right panel excludes transport and chemistry time; its favorable logarithm does not overcome the left panel or inlet mass limits.

11. Soft-to-hard transduction and physical attainability

The preferred sequence is an information-rich porous scaffold, selective recruitment, material conversion while diagnostic/service routes remain accessible, functional correction, passivation or fusion with a reserved drift margin, and selective scaffold release. Geometry can be molecularly patterned at critical interfaces while the bulk is formed by conventional deposition, crosslinking, or mineralization.

No scaffold can create absent elements. Stoichiometric conservation restricts all products to the elemental inventory of the supplied reactants; the reaction network also restricts accessible oxidation states, phases, interfaces, and temperatures. A finite material alphabet can be useful without being chemically universal.

The practical progression is one scaffold with one inorganic material; then one inorganic conductor plus a stable dielectric/support; then independently addressable material channels and tested interfaces; then a passive device; and only afterward increasingly complex functions. Semiconductor doping profiles, low-defect single crystals, grain-boundary mobility, optical losses, thermal expansion, and high-temperature densification are separate problems. A DNA-compatible reaction bath is not a universal materials process.

DNA-programmed inorganic frameworks and subsequent device integration provide relevant component evidence [P10, P11]. Macroscale-area DNA-framework patterning also exists with substantial external patterning [P12]. These results support selected routes from programmed soft structures to inorganic function. They do not demonstrate autonomous, seed-only, self-repairing multimaterial growth at centimeter scale.

11.1 The precise transfer from the 3-D conductivity research

The inspected v6 conductivity manuscript [U5] distinguishes an actual physical response image from arbitrary algebraically admissible spectra, and distinguishes approximation by a sequence from exact realization by one cell. We retain that discipline. Its infinite hierarchy is not invoked as an efficient finite fabrication compiler.

For a gray coefficient P between zero and one, let m be its mean and B its binary unsaturation integral, the integral of P(1-P). The inspected exact-volume rounding argument gives a binary coefficient chi of required fraction theta with:

$$\|P - \chi\|_1 \leq 2B + |m - \theta|.$$

Proof reconstruction. At equal fraction theta = m, selecting the largest m fraction of P gives at least the overlap obtained by the fractional selector P itself. Expanding the L1 error therefore bounds it by 2 times the integral of P(1-P). Altering the selected set by volume |m-theta| gives the stated general bound. This is an elementary rearrangement argument; stronger sharp bounds are retained in [U5].

For positive real conductivity contrast confined to a compact uniformly elliptic range, a variational higher-integrability argument gives constants C and alpha > 0 with response perturbation at most C times that L1 error to the power alpha. The proof compares energy minima using each other's correctors and uses a geometry-uniform higher-integrability estimate. The constants deteriorate with contrast and operating regime. The result does not reach perfect zero-conductivity voids uniformly.

This supplies a useful design certificate: a surrogate gray design is not accepted solely because its simulated spectrum looks right; it also carries a bound to an actual binary realization. It does not prove that chemical deposition implements that rounding, that a periodic homogenized tensor certifies a small finite module's boundary response, or that the constants are practical. The proposed device must still be measured through its actual ports after transduction.

12. Physical architecture and its unbuilt components

The shortest plausible architecture uses a temporary manufacturing layer surrounding or interpenetrating the final material. This layer carries local state, reagents, diagnostic connections, and sacrificial reserve paths. The final structure can remain simple. Trying to embed the entire controller, chemistry library, and repair machinery inside every final atom is unnecessary and implausible.

Required operation	Plausible initial implementation	Boundary of current evidence
Seed-dependent information growth	Seeded DNA tile or related programmable assembly in a controlled bath	Algorithmic growth is established; the present complete 3-D grammar is not chemically compiled.
Local finite state and gates	DNA strand-displacement motifs; larger electronic or microfluidic controllers at first	Sequence orthogonality, copying reliability, and long-lived state are not supplied by the abstract alphabet.
Structural bulk	Crosslinked scaffold, silica/mineral support, recruited particles	Shrinkage, strain, mechanical integrity, and inaccessible pores must be measured.
Conductive differentiation	Local particle recruitment and compatible metal deposition	Conductivity, contact resistance, leakage, and thermal stability depend on the actual chemistry.
Functional diagnostic	Permanent or temporary electrical ports, initially external instruments	Connected modules require isolation or an explicitly solved loading model; ideal local sensors are an assumption.
Bounded reserve repair	A porous spare path receiving measured increments of deposited material	Monotone, reproducible conductance increments without damaging neighbors are the decisive unbuilt actuator.
Local closure coordination	Compartment/controller acknowledgement; later molecular signaling	The simulations assume correct message identity, version, and transmission.
Final locking and release	Compatible passivation, crosslinking, scaffold removal	The final response drift must be bounded, or measurement and repair must remain available afterward.

The most credible first device is a low-frequency passive electrical or fluidic network with a small number of ports per module. A diode, transistor, photonic resonator, or mechanical actuator requires a different behavioral contract. Linear elasticity can use a similar energy argument only within a stable coercive regime, with rigid modes, prestress, buckling, and contact handled explicitly. Complex optical/electrical responses generally lack the real Loewner ordering used in R1; a small-signal frequency-domain extension needs its own proof.

Local physics-driven adaptation of resistor and elastic networks is prior art [P3, P4, P5]. The proposal here is to use a developmental scaffold and disposable manufacturing resources to build, test, correct, and then mature material modules under explicit compositional certificates. The simulations do not show that this beats an equally capable conventional local controller.

12.1 Maintenance and what biology does not supply

The same program can maintain a device only if the relevant references, observable ports, transport paths, repair stock, and compatible actuators survive operation. A sealed two-terminal response alone records no unique microscopic blueprint; many different interiors have the same response. Maintaining function may use a reserve bypass without reconstructing the original bonds. Restoring a specific damaged interior instead requires additional information and access.

With ongoing damage, a finite reserve eventually exhausts unless it is replenished or modules are replaced. A mission-time guarantee must include the number of future inspection opportunities, common-reference survival, wear, and the last repairable state. The fabrication confidence budget cannot be reused indefinitely as a lifetime budget. Experimental replication-like operations should remain confined to the controlled scaffold/process vessel; no autonomous organism or uncontrolled replicator is required by this architecture.

Biology establishes the physical possibility of hereditary information, local differentiation, distributed chemistry, growth, and maintenance. It does not provide arbitrary inorganic phases, high-temperature processing, semiconductor-grade interfaces, fast dry manufacturing, or an engineering proof of yield. The proposed passive module contracts and material-conversion schedule are defined by physical response and compatible chemistry, not by renaming a genome or copying an organism.

13. Computational evidence and reproducibility

13.1 What the v2 model implements

The new target is a nonperiodic passive-conductance family on a fixed 2-D or 3-D nearest-neighbor scaffold. It has 64 sites and 112 edge modules in 2-D, or 125 sites and 300 edge modules in 3-D. Each edge module contains three parallel branches, each containing two series bonds, and one available parallel reserve branch. The output roles vary by inherited parity state and orientation. This is internal functional differentiation, not a new demonstration of Brownian molecular geometry formation. The earlier package retains irregular 2-D and 3-D growth shapes.

The blueprint baseline has idealized identification of the modeled pre-conversion bond faults; it is deliberately strong in that respect. Full replacement-bond material, discarded bonds, and delivery time are charged. Initial bond faults occur with probability 0.12 and reduce a bond by a factor 0.15. Conversion faults occur with probability 0.08 and reduce a bond by a factor 0.12. A spatial half-region may have its body and local bond reference scaled together by 0.65, with object-level probability 0.35. The separate terminal contract reference is intact in the main runs. The biased-reference condition violates that last premise deliberately. Neither model corrects a fully corrupted common root that changes both the intended target and every independent diagnostic.

Post-conversion terminal measurements use the finite-confidence procedure in R4. Reserve increments are 0.045 of target conductance times a bounded random multiplier between 0.6 and 1.4. The maximum reserve is 0.9 of target conductance. All methods are allocated the same reserve capacity and service geometry; unused reserve is still physical design overhead. Added active material is charged correctly as two equal series bonds: obtaining extra module conductance G requires total bond conductance 4G, matching the path-length convention of the nominal module. A one-edge shortcut is not used to underprice repair.

Each node maintains local readiness and waits for child acknowledgements before closing. Feedstock demand is checked against root and every service-edge capacity. The electrode network is solved only after the simulated manufacturing dynamics to score final object function. The repair controller sees a local terminal measurement and its local contract, not the final global conductance score or a bond-by-bond target oracle.

Important idealizations remain: inherited coordinates and references, the fixed oriented scaffold embedding, electrical port isolation, bounded incremental deposition, no hidden coupling outside the ports, a calibrated seal envelope, and routable service channels. Molecular species count and thermodynamic energy remain unspecified. The manuscript's physical conclusions are limited accordingly.

13.2 Preserved v2 results: 512 default runs

There are 32 independently seeded objects per condition and dimension. The pass criterion is completion plus final global conductance within 8% of target. The same fabrication draws are paired across methods. The two target sizes are not directly comparable measures of scalability. Mean conductance ratios below include unfinished objects where indicated; they are diagnostic scores, not manufactured yield.

Condition	2-D completed function	3-D completed function	Interpretation
Open loop	0/32	0/32	No functional repair after conversion.
Blueprint repair before conversion	0/32	0/32	Local body-reference repair cannot remove later conversion errors or shared reference errors.
Blind fixed reserve addition	1/32	1/32	Actuation without matched diagnosis is inadequate for this fault distribution.
Diagnostic only	0/32	0/32	Correctly refuses to complete many defective modules.
Response repair with early sealing	0/32	0/32	Premature closure strands unresolved descendants.
Response contracts plus access	32/32	32/32	Every final local response also meets its declared envelope.
Conventional joint controller	32/32	32/32	Same capabilities and policy; ties exactly, including cost and time.
Shared 7% diagnostic gain bias	6/32	0/32	12 and 4 objects respectively finish with invalid local certificates.

The response-contract method's mean conductance ratios are 0.96787 in 2-D and 0.96694 in 3-D, with sample standard deviations 0.00245 and 0.00172. It intentionally stops inside the acceptable band; it is not trained to reproduce exactly 1.00000. Open-loop means are 0.65293 and 0.58814. Blueprint-repair means are 0.79794 and 0.70841.

These numbers are not a head-to-head improvement over v1's 2/8 reference functional successes. The new and old models have different targets, physical abstractions, tolerances, and repair operators. The controlled causal comparisons are the paired conditions inside the present experiment.

Nominal functional material is 39.2 and 113.6 model units. The response method adds means of 10.70773 and 38.77344, or about 27.3% and 34.1%, excluding the separately charged scaffold. Mean inspection sample counts are 12,681.5 and 41,250. Mean maturation rounds are 28.25 and 28.78. Total scheduled times are 263.78 and 764.03 abstract units, versus 245.47 and 709.05 for open loop. The matched conventional controller has exactly the same outputs and costs. These figures are neither seconds nor a calibrated molecular energy budget.

All 32 successes in a condition give a two-sided exact 95% binomial interval with lower endpoint about 0.891, not proof of yield one. The synthetic distribution and strong actuator assumptions limit extrapolation more than this sampling interval does. No enormous-N physical reliability claim is inferred from these runs.

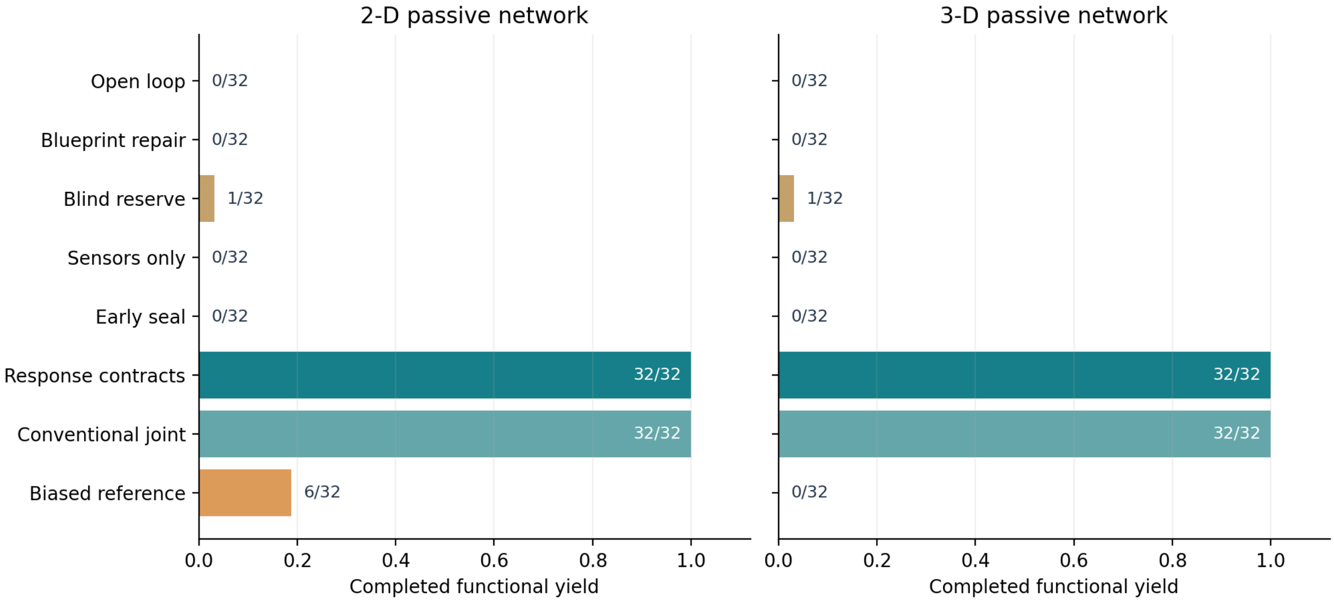

Figure 5. Functional yield is conditional on the reduced model's stated hardware assumptions. The conventional matched baseline ties the response-contract controller; the evidence supports the proposed mechanism and certificate logic, not exclusive algorithmic superiority.

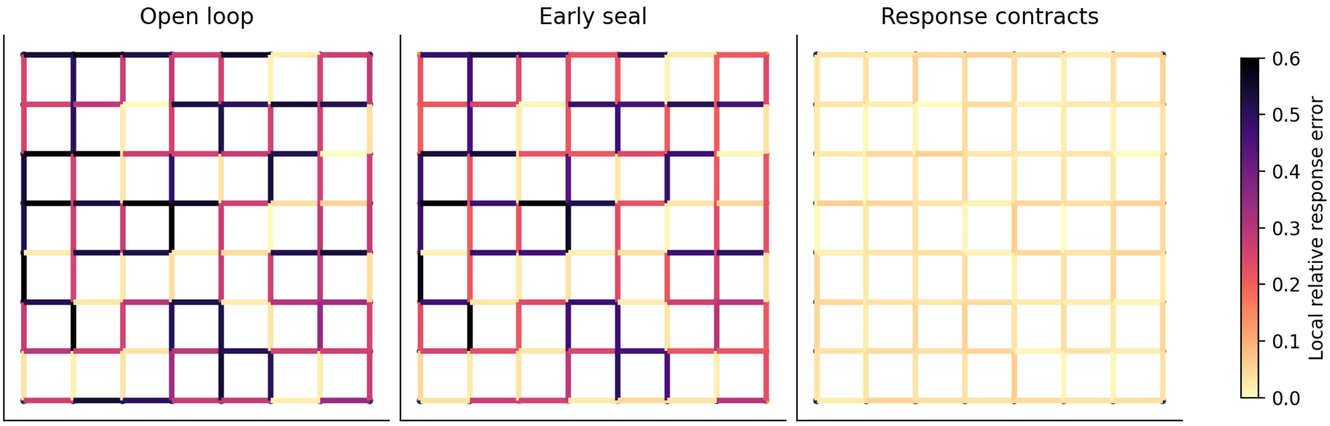

Figure 6. One paired 2-D fabrication draw. Edges show local relative response error; node state distinguishes sealed and unsealed regions. The colored geometry is a finite network simulation, not a microscopy image.

13.3 Negative controls and theorem checks

An additional 32 seal-stress runs retain the nominal 1% certificate margin but allow actual independent seal changes up to 18%. Every object finishes with some invalid local certificates; mean local contract satisfaction is only 0.4587. Nevertheless all 32 global conductances remain within 8%, ranging from 0.93296 to 0.98729 of target. This is not a contradiction: the local contract is sufficient, not necessary, and partially cancelling random changes can preserve one global response. A correlated downward seal shift can instead fail the object. A single passing whole-device test cannot validate an assumed local envelope.

Numerical checks include 300 correlated multiport composition instances, 250 random positive-conductance energy bounds, and 400 noncommuting evidence/control calculations. No asserted inequality is violated. The direct quadratic optimum and formula agree to maximum absolute error 3.55e-15. The single-probe counterexample has zero first-probe current difference and relative eigenvalues 1/3 and 1. These checks are reproducible and are not substitutes for the proofs.

Sixteen research tests pass, including Kron elimination, seal margins, local routing, postorder access, a channel bottleneck, zero-sensor/zero-actuator limits, matched subspaces, insufficient reserve, the conventional-controller tie, and the integrated material ledger. The original v1 code, data, manuscript, and limitations are retained under `baseline_v1`. Its 96 default and eight diffusion-stress runs are historical baseline evidence, not new v2 runs.

13.4 Remaining v2 computational extensions

The next implementation should couple the actual v1 concentration field to finite-rate reserve deposition, replace ideal reference copying with a coded communication model, include contact/isolation errors, model reaction cross-talk and strain, and permit local module rejection/replacement. It should test multiple independent terminal patterns on multiport devices and report false acceptance under biased or drifting sensors. These are concrete missing mechanisms. Their absence must not be hidden by calling the current fixed-network simulator physically complete.

13A. New v3 experiments and what they establish

13A.1 Controlled changes from the v2 model

The new suite uses the same nonperiodic nearest-neighbor role grammar and grown service-tree geometry: an 8 by 8 planar network with 112 scalar modules and a 5 by 5 by 5 spatial network with 300 modules. Each module is represented by its post-conversion scalar response, initially uniform on [0.65,1.35] in witness-relative units. This bounded disorder model is specified, not fitted to laboratory material data. The v2 microscopic bond-error model and absolute conductance objective are different, so their yields are not directly comparable.

The v3 nominal target has four external ports. Success requires completed manufacturing and projective response error at most 0.04; the internal voltage map under a unit boundary drive is scored separately. Two-terminal scale equivalence would be vacuous and is not the test. The local G3 log tolerance is 0.04; remaining seal error is bounded by 0.005; diagnostic radius is approximately 0.006; deposition increments lie in [0.007,0.012]; available reserve is 1.05 per module; and the inspection horizon is 128.

The comparison graphs have 293 and 1,186 edges. A stable, absolutely uncalibrated witness is attached by one extra link. Local paired observations share detector gain. Fresh ratio log-errors are independent Gaussian with single-sample standard deviation 0.012. A simultaneous failure budget of 0.005 requires 326 samples per pair in 2-D and 218 in 3-D. Matching schedules use seven and twelve nonoverlapping probe slots respectively. The one-witness resistance maxima are 2.61535 and 1.64203, which explain why the smaller 2-D object needs more repeats per edge.

Every ensemble inference checks its normal-equation residual, using a conservative grounded-inverse and standard-roundoff allowance. The resulting numerical log-error bound is required to stay below 0.00000001 and is included in the diagnostic radius. This is a floating-point error audit under the declared arithmetic model, not a proof-assistant or interval-arithmetic certificate.

The manufacturing ensemble uses a finite factored estimator; the separately executed local-message estimator provides an implementation route and a measured algorithmic round count. Its latency is deliberately excluded from the ensemble's service-and-acquisition time subtotal. Those subtotals are not total fabrication times. The model preserves material delivery capacity, finite growth layers, diagnostic sampling costs, bounded reserves, and local postorder final closure, but it does not solve diffusion, hydraulics, chemical kinetics, Brownian alignment, or molecular control errors. No new molecular species count or energy measurement is claimed.

13A.2 Results from 512 new paired manufacturing runs

Each of eight conditions uses the same 32 underlying initial-state seeds in each dimension. Methods within a seed are correlated comparisons, not additional independent worlds. A completed object is not scored as successful merely because its controller says so: the final four-port response is independently computed from the final physical conductances after sealing.

Condition	2-D functional completion	3-D functional completion	False local certificates, 2-D / 3-D
Projective reserve repair	32/32	32/32	0 / 0
Shared detector gain varied per pair/epoch	32/32	32/32	0 / 0
All material conductances multiplied by 0.6	32/32	32/32	0 / 0
Equally capable conventional ratio controller	32/32	32/32	0 / 0
Fixed unit-scale representative	0/32	0/32	0 / 0
Reserve reduced to 0.4	0/32	0/32	0 / 0
Spatial differential comparison bias	0/32	0/32	29 / 7
Witness link removed before completion	0/32	0/32	0 / 0

Shared detector gains ranged from exp(-0.7) to exp(0.7) and canceled in the paired ratio. The common-material-scale condition also scales the witness and available conductance increments. It verifies the stated symmetry; it is not a test of arbitrary changes to material chemistry. The equally capable conventional controller has the identical policy by construction and ties. This comparison does not establish superiority over conventional ratio control, lithography, or printing.

The fixed-representative condition is conservatively rejected by the local feasibility gate because some modules already exceed its allowed conductance. It is not a comparison against every possible conventional fabrication strategy; replacement, subtraction, or a different global certificate could change the result. The insufficient-reserve case is also rejected honestly before repair.

For the projective policy, mean projective response errors were 0.002221 and 0.001779 in 2-D and 3-D. The worst among all 64 positive baseline runs was 0.005852. Mean maximum absolute voltage-map errors were 0.002015 and 0.002296 for a unit drive; the worst was 0.003493. These are synthetic endpoint scores under the declared static conditions.

Mean added-material proxies were 11.4985 and 33.6441, about 29.3% and 29.6% of nominal functional-network material. These proxies use the inherited 0.4 material units per normalized conductance unit; they are not grams or measured deposition energies. Allocated reserve capacity is 105% of nominal functional conductance and is larger than the material actually consumed. Empty reserve geometry, comparator hardware, contacts, and the stable witness also occupy real space and are not assigned measured fabrication costs here.

Mean inspection counts were 68.3438 and 69.3438. The conservative strategy acquires roughly 6.53 million and 17.93 million completed ratio samples per object. Its mean service-and-acquisition time subtotals were 454.27 and 968.48 in the model's arbitrary time units, excluding inference and reduction latency. This is a substantial control-resource cost, not evidence that nanoscale manufacture is already fast.

The final absolute conductance ratios averaged 1.2912 and 1.2947, although the prescribed projective function passed. Under a common material factor of 0.6 they averaged 0.7747 and 0.7768, while the voltage map and projective errors were unchanged to numerical precision. These deliberately different absolute conductances make the allowed specification change transparent. A 32/32 outcome alone has an exact two-sided 95% binomial lower confidence endpoint near 0.891; it does not establish unit population yield.

The differential-bias test adds a gradient-shaped log error spanning -0.15 to +0.15 across the object. Of its 64 runs, 36 completed with false certificates and failed the independent projective test; 28 exhausted their reserves. Mean cycle-residual energies remained nearly the same as the unbiased cases. The separate noiseless counterexample recovered a wrong field with maximum bias 0.15 and cycle residual approximately 0.00000000000000214. A passed cycle check cannot validate this failure mode.

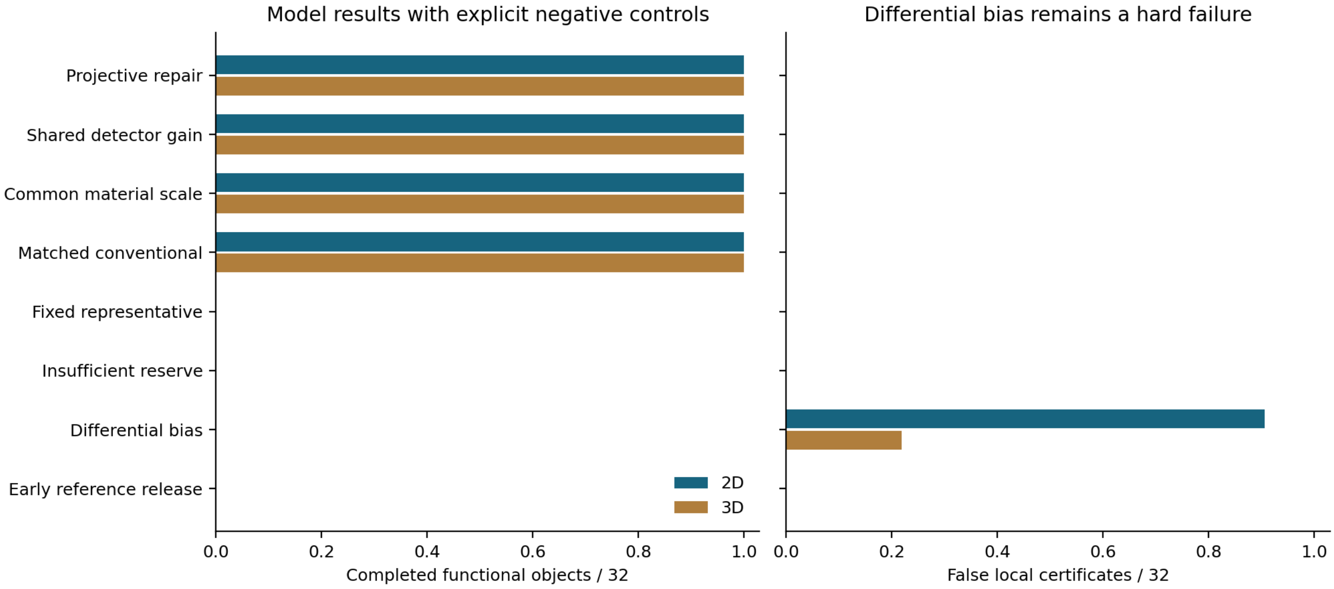

Figure 7. The new positive cases and mandatory negative controls. Incomplete objects contribute to neither functional completion nor false accepted certificates. The matched conventional condition is an exact policy tie, not an independent invention.

13A.3 Numerical checks, local execution, and the reserve transition

The package includes 28 passing research/software tests: the original 16 and 12 new ones. New checks include 80 independent linear-program comparisons of G2 feasibility and minimum material, 500 adversarial endpoint-noise constructions for G3, covariance identity, common-scale cancellation, an invisible differential-bias example, the local solver's residual bound, and reference-access failure. Floating-point tests are not formal interval proofs.

The G4 formula was checked against 100 independent numerical integrations; the largest absolute disagreement was about 0.0000000000000197. Two hundred four-port passive-network tests satisfied G1, with the largest projective error about 0.014934, below 0.04. Six thousand independent noise-field draws tested the calibration covariance; the largest relative sampling deviation among the tested diagonal variances was 4.32%, compatible with this finite Monte Carlo check but not a formal distributional calibration test.

The phase experiment sampled 25,000 arrays: 5,000 each at sizes 4, 16, 64, 256, and 1,024. Each array was evaluated at 31 capacities, producing correlated evaluations within a size. At reserve 0.55 the 64-module result was 295 successes in 5,000 arrays, against an exact probability of

0.060415. At reserve 0.60 all arrays were feasible, as the support-wide theorem predicts. The worst empirical-versus-exact probability difference over the reported grid was 0.01298. The transition was derived before these computations; it was not inferred by fitting a curve.

The comparison-topology study uses ordinary 1-D, 2-D, and 3-D nearest-neighbor boxes. At 128 nodes in 1-D the worst effective resistance was 127; at a 16 by 16 grid it was 3.60852; at an 8 by 8 by 8 box it was 1.27912. These illustrate established dimension-dependent calibration behavior [P15], not a newly discovered dimension law. All simulations are reproducible from stored seeds, parameters, and code; no laboratory measurements were introduced.

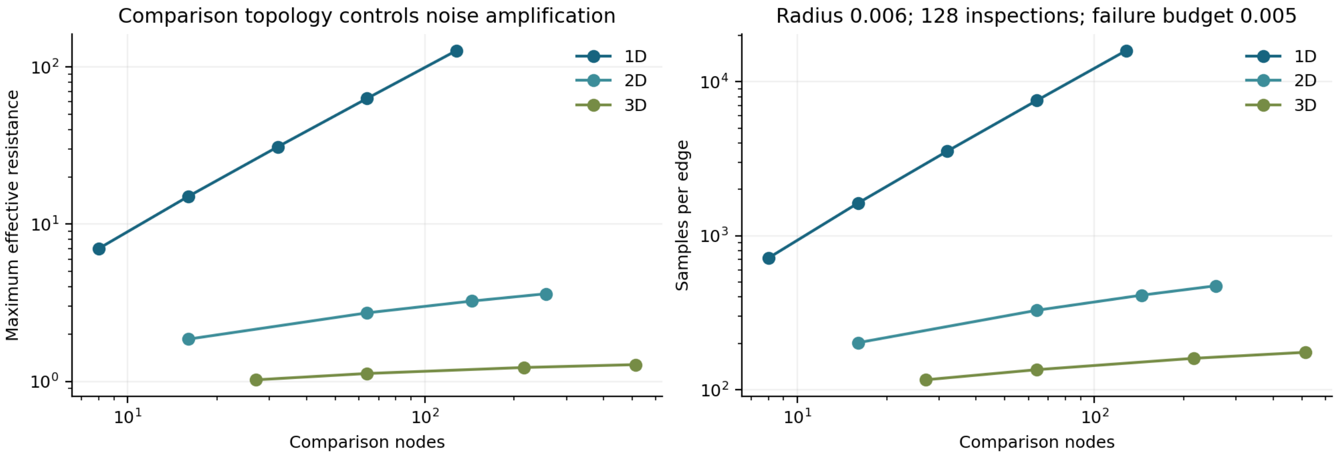

Figure 8. Finite-box effective resistance and the sample count needed for the same simultaneous log-error radius. More dimensions help only when the comparison graph supplies the corresponding independent routes. Local solution time remains a separate constraint.

14. The v2 minimal decisive experiment

The smallest useful wet experiment is a **four-module passive conductor/dielectric array with separately addressable service paths, post-conversion electrical probes, and a bounded spare deposition path per module**. A 10-100 micrometer compartment scale with finer DNA-directed or other programmable substructure is an initial design target, not a claimed current manufacturing capability. A generic chip holder and its electrodes are apparatus; any target-specific patterning must be charged explicitly.

The first objective is to test the new maturation principle, not to combine every unsolved operation at once. Form the same four module templates using one fixed compatible scaffold/deposition chemistry. Include deliberate weak links after the nominal conversion stage. Measure the module's full relevant response, apply incremental reserve deposition while its service path remains open, and close only after the response and descendant obligations pass. Preserve a terminal measurement after closure to assess the actual seal drift.

Use a paired factorial design: diagnostic-guided versus blind deposition, crossed with service retained versus early closure. Include an equally informed conventional controller. Use two target-response programs on the same holder to separate target programming from fixed apparatus patterning. A preliminary electronic resistor-board implementation can validate the message protocol cheaply, but counts only as a control experiment, not nanofabrication evidence.

Before running the wet comparison, calibrate the attainable increment range, reserve capacity, sensor bias, electrical isolation, reagent transport, and post-seal response distribution on separate specimens. Choose eta and the error budget from those data and a real device requirement; do not force the simulation's 8% and 1% values onto an incompatible chemistry. Use fresh calibration and test specimens, randomized condition assignments, and blinded final electrical scoring. At least

20-30 independent arrays per principal condition would reveal large mechanism effects; precise high-yield claims require a separate power calculation and substantially more samples.

Support for the central claim: retained diagnostic and repair paths permit post-conversion weak links to reach the prespecified terminal envelope; the local contracts predict the connected array's full declared response; early closure blocks otherwise attainable correction; and measured resource costs are within the stated capacities.

Falsification of the proposed implementation: reserve growth is nonmonotone or uncontrollable at the required resolution; selectivity produces hidden shorts; closure drift exceeds every practically useful margin; probes change the object enough to invalidate their result; or the paired method has no acceptable material/time tradeoff against the matched conventional baseline.

Alternatives to exclude: unmeasured external retuning, deposition everywhere rather than targeted correction, direct lithographic encoding of the target, changing the acceptance threshold after seeing results, and treating multiple measurements of one object as independent manufactured samples.

An experimentally demonstrated four-module instance would validate an important interface between programming, conversion, functional correction, and closure. It would not validate the conditional active-macrocell universality theorem. The next experiment must then implement seed-controlled geometry/state propagation and the local closure signal on the same material platform.

14.1 Priority by value, cost, difficulty, and information gain

Priority	Experiment	Relative cost and difficulty	Information gained
1	Independent finite proof/code audit and biased-sensor counterexamples	Low laboratory cost; moderate mathematical effort	Detects logical errors before choosing chemistry.
2	One-module deposition, metrology, and seal calibration	Moderate; requires compatible chemistry and electrical contacts	Determines whether the central actuator and final-change window exist at all.
3	Four-module paired repair/access test	Moderate to high; routing and probe isolation are harder	Separates diagnostic value, repair value, and closure failure.
4	Seed-controlled state propagation on the same substrate	High molecular-design effort	Tests whether the target resides in the seed rather than the apparatus.
5	Larger 3-D perfused device	Very high integration effort	Measures the true transport, strain, interface, and reference scaling limits.

These are relative planning estimates, not supplier quotations or promised timelines. Attempting the larger device before finding a reproducible one-module correction window has low expected information gain per unit effort.

14A. The decisive v3 experiment

Use four post-conversion conductor modules arranged as a resistive bridge with separately accessible terminals and independently bounded parallel reserve paths. Choose nonidentical nominal conductances, for example proportional to 1, 2, 1.4, and 0.8, so the intended voltage output is not a trivial zero signal. The bridge output is then about -0.30303 of a unit top-to-bottom drive under the declared branch orientation. Preserve a generic pair-comparison frontend and witness until all modules complete.

The first gate is a benchtop electronic emulation with switched passive resistors. It can decisively test the numerical representative selection, budgets, paired-gain cancellation, and reference-release logic. It cannot validate the proposed material backend. The second gate substitutes an actual scaffold-compatible post-conversion incremental deposition actuator, characterized before its use in the growth experiment.

Compare projective representative selection against a fixed representative and a matched conventional ratio controller. In separate conditions, vary shared detector gain, deliberately introduce differential arm error, remove the witness link early, and cross the measured reachable-reserve boundary. Verify final function with an independent instrument and the full four-port response under three independent grounded excitations. Measure deposited material, rejected modules, electrode/contact drift, and every intervention. The controller must not receive the final evaluator's conductance ground truth.

G2 is supported if measured reachable intervals predict feasible versus infeasible target bands and the minimum-material endpoint agrees within measurement/actuation error. It is falsified for a proposed backend if coupling, nonmonotone growth, discontinuous percolation jumps, or unstable contacts invalidate those intervals. G3 is supported only after its bounded noise, step, capacity, access, and seal premises are measured. An apparent counterexample with violated premises falsifies that backend or parameterization, not the mathematical implication.

G4 requires a separate ensemble across module counts and controlled bounded disorder. Four modules can test exact reachability and the boundary mechanism; they cannot establish an asymptotic transition. A scale study using 4, 16, and 64 switchable modules is a relatively inexpensive next stage. Replacing those controls by chemistry is a later gate. Sample sizes should follow a prospective power calculation after noise characterization; a few successful bridges cannot establish high-yield manufacture.

The highest-information negative control is differential bias with a small cycle residual. If the physical system detects it, identify which additional information breaks the G5 ambiguity. If it does not, bound its frequency or keep the corresponding calibration requirement. Neither outcome supports a self-certifying absolute nanofabricator.

15. Implementation ladder and functional benchmarks

Stage	Smallest informative milestone	Main acceptance criterion
Simulation	Couple chemistry-rate, transport, reference faults, and reserve control	Conservation, causal local decisions, calibrated comparison, and held-out failure tests.
DNA-like substrate	Two seeds generate distinct nonperiodic local states from a fixed feedstock set	Seed dependence and measured local misbinding/copy-error rates.
Hybrid scaffold	Add one structural and one functional recruited component	Measured selectivity and stable geometry through both stages.
Material transduction	Four-module correction-and-seal experiment	Post-conversion response correction and validated final-drift bounds.
Functional device	Small passive sensor or flow/impedance network	Function over all declared input/load conditions, not only a shape image.
Millimeter scale	Interior supply plus local reference and repair continuity	No starvation/occlusion, measured stress and heat, realistic yield/time.
General platform	Reusable physical compiler backend over several compatible module classes	New target families without a new unique molecule or mask per output location.

Functional benchmarks should be declared before fabrication. Level 0 is a periodic lattice, with occupancy and lattice-defect statistics. Level 1 adds a nonperiodic 3-D boundary with Hausdorff or voxel-distance tolerance. Level 2 adds internal material-label fidelity and interface placement. Level 3 is a multimaterial passive response with specified port matrix and operating range. Level 4 adds a mechanical or optical function such as resonance frequency, quality factor, load range, or optical spectrum. Level 5 requires electrical function, isolation, contacts, stability, and power handling. Level 6 combines sensing and actuation with calibrated response and cycle life. Level 7 requires multiple interacting subsystems and verification under joint operating conditions.

Success at a higher level does not excuse failure of essential lower-level constraints. Conversely, a passive device can have excellent functional performance despite some microscopic departures from a nominal CAD file. This is the function-versus-coordinate distinction on which the restricted theory relies.

16. Numerical scaling from 100 nanometers to 1 centimeter

The following table counts 20-nanometer cubic scaffold units in a dense cube and gives bare diffusion times. The feature pitch is an illustrative accounting unit, not a demonstrated controllable primitive at every location. At the smallest sizes a continuum diffusion estimate is only an order-of-magnitude guide.

Object side L	Units at 20 nm pitch	L squared/D, D = 1e-9 m squared/s	L squared/D, D = 1e-11 m squared/s
100 nm	125	1e-5 s	1e-3 s
1 micrometer	125,000	1e-3 s	0.1 s

Object side L	Units at 20 nm pitch	L squared/D, D = 1e-9 m squared/s	L squared/D, D = 1e-11 m squared/s
100 micrometers	1.25e11	10 s	1,000 s
1 mm	1.25e14	1,000 s	100,000 s
1 cm	1.25e17	100,000 s	10,000,000 s

For example, (0.01/20e-9) cubed equals 1.25e17 units. Individual nanometer-level address control for all these units is implausible. A 10-micrometer module pitch instead gives one million modules in a centimeter cube. Such modules could contain many nanoscale features while retaining a bounded number of functional/service interfaces. The module itself and its resource capacity still need fabrication and validation.

At an illustrative scaffold-front speed of 1 micrometer per minute, one centimeter requires 10,000 minutes, about 6.9 days, even before other process stages. This is a conditional arithmetic example, not a claimed measured developmental growth speed. At 1 millimeter per hour, the same traverse is ten hours but needs a different, plausibly mesoscale process. The causal front and material conversion steps can have very different rate constants.

A dense 1-cubic-centimeter part of density 2 grams per cubic centimeter requires 2 grams of material. Supplying this in 24 hours requires about 23 micrograms per second of incorporated material. At 10 grams per liter of usable precursor, it requires roughly 2.3 microliters per second of feed, or 0.20 liters in a day, before accounting for incomplete conversion and waste. The 10-micrometer-radius channel example above carries about 0.039 microliters per second: about sixty such full-length channels would be required for that nominal flow, with pressure loss, branch distribution, and solid loading still to be included. More dilute feedstocks make the flow burden correspondingly larger.

For one million modules, 48 inspection opportunities, scalar noise sigma = 0.01, and a desired measurement radius w = 0.01 at risk 0.01, the elementary concentration formula requires at least 46 independent samples per opportunity. This is only a scalar noise calculation. Multiport matrix dimension, poor conditioning, drift, and correlated noise can make diagnostics much more expensive. The total number of samples can be large even when each module samples in parallel.

Thermal expansion and densification require separate scaling. A free strain of 1% across 1 cm is a 100-micrometer dimensional change, far above a nanometer tolerance. Constraint can turn that shrinkage into stress or cracking. Hierarchical compliant joints, staged conversion, and compensated geometry may help, but no theorem here makes strain disappear. Critical interfaces need their own process-compatible microscopic components.

16.1 Additional v3 scaling costs

The v3 reduction removes an absolute reference requirement for a scale-free function; it does not remove O(R) generic comparator sites, accessible reserve space, or temporary state. A regular three-dimensional comparison network needs order log(RH/delta) repeated samples per local edge at fixed error radius, hence order R log(RH/delta) total samples per inspection. The graph must remain connected and sufficiently well supplied. The common witness needs stability, even though its absolute conductance need not be known.

Sequential neighbor relaxation has a different scaling: on a regular box of side n it takes order n squared times a precision logarithm. If a hypothetical 1-cm object used 100-micrometer modules, it would have n = 100 and approximately one million module positions. With an assumed 1-ms local update time and a logarithmic factor of 14, a simple diffusion-like solve would take order 140 seconds per inspection before constant factors and acquisition time. Seventy inspections would be order 2.7 hours of inference alone. At a 10-micrometer module pitch, the n-squared term is one hundred times larger. These are illustrative scaling calculations, not predicted device timings.

Hierarchical calibration, physically fast analog relaxation, parallel module replacement, or fewer diagnostic epochs may improve that cost. They must preserve noise and service certificates and be demonstrated; no assumed exponential communication speedup is charged to the present result. Applying a comparator to every atom is excluded. Functional modules must be sufficiently large and response-simple to amortize the control apparatus.

A common conductance scale changes dissipated power under voltage drive. If thermal or current constraints impose a scale interval, that interval re-enters G2 and needs physical calibration. Functional gauge freedom cannot hide an impossible power budget. A witness that remains stable in a benchtop bridge may drift during centimeter-scale mineralization, drying, or heating, so beta and the diagnostic-error budget must be measured across the actual maturation history.

17. Failure modes, prior art, and adversarial audit

17.1 Failure modes that invalidate the positive theorem

Failure	Consequence	Required repair or honest boundary
Common seed/reference corruption	Material and checker agree on the wrong target	Independent calibrated reference and charged root-error budget; local consensus alone is insufficient.
Incomplete multiport probes	Hidden response modes can be wrong	Complete probe basis or a proved restricted subspace contract.
Irreversible last-step damage	Pre-seal certification expires	Bound the change, inspect afterward with remaining repair, or reject.
Hidden intermodule coupling	Local contracts no longer compose by R1	Enlarge modules/contracts or model the coupling explicitly.
Port/contact changes during assembly	Tested module differs from installed module	Include contacts as modules and test them in the relevant installed regime.
Early closure or exhausted feedstock	A mathematically correct repair action is unreachable	Access acknowledgements plus capacity and resource checks.
Uncontrollable deposition or exhausted reserve	R3's finite reachability fails	Smaller bounded increments, broader actuation, local replacement, or declare the target infeasible.
Near-zero conductance or high contrast	Poor measurement conditioning and weak continuity bounds	Coarser tolerance, different module geometry, or a stronger diagnostic; no uniform near-percolation guarantee.
Genome/state copying errors	Wrong region identities or false acknowledgements	Explicit communication coding and anchor mechanisms, unimplemented here.
Chemical cross-talk, aggregation, or kinetic trapping	The abstract local transition model is wrong	Redesign chemistry and measure rates; do not patch a wrong physical model with a confidence label.

17.2 What is and is not different from existing paradigms

Algorithmic tile assembly already links programs, seeds, finite alphabets, and nonperiodic growth. Proofreading tile sets already address assembly errors [P8, P9, P13]. DNA framework templating already connects programmable structures to inorganic materials [P10-P12]. Physical learning already uses local responses to tune material function [P3-P5]. Spectral approximation, Kron reduction, and local certificate schemes already support mathematical components of the present proof [P1, P6, P7].

The candidate contribution is the **combined fabrication specification**: a compressed geometry/program layer; measurable response contracts that compose without a per-module error sum; matched diagnostic/repair reserves priced using the author's earlier research; closure conditioned on both function and descendants' access; and a final material-change budget. The v1 redundancy-access reversal is retained as a transport constraint. No searched source establishes independent priority for this exact combination, and the present search does not prove it absent from prior work.

The architecture can use parallel local chemistry where serial atomic placement would require enormous instruction throughput. It has no established general speed or cost advantage over conventional additive manufacturing, lithography, or staged self-assembly. Those methods also exploit bulk chemistry, repetition, masks, and parallelism. Developmental fabrication's potential advantage arises only for target families with reusable generative structure and reliable local execution under a favorable apparatus/material budget. It may be worse for a small batch of arbitrary intricate parts.

17.3 Final adversarial questions

Where is global design information stored? In the target genome, its initial symmetry-breaking seed, and any charged target-specific environment; the local interpreter and generic hardware are separately accounted for. Is complexity hidden in species? The chemical species number is not claimed; macromolecular sequence diversity and state machinery remain explicit implementation barriers. Does error accumulation kill large objects? R6 avoids a per-atom perfect-yield requirement under its functional, measurement, and last-seal premises; it does not protect an unbounded common failure mode.

Does diffusion kill centimeter growth? Unvascularized supply can be extremely slow; the object needs a physically sized service network and sufficient boundary flux. Can interiors receive feedstock? The local tree rule preserves routes, and the capacity ledger prices delivery; a real hydraulic network remains to be engineered. Can materials actually be incorporated? Selected scaffold-to-inorganic routes are supported by prior work, while controlled repeated reserve deposition and final drift are the decisive missing experimental capabilities.

What prevents kinetic traps? Reversible assembly windows, local rejection, and staged conversion are proposals; chemistry-dependent rate measurements must demonstrate them. What handles defects after hardening? Only surviving diagnostic/control resources or a separately validated passive tolerance; an inaccessible hard object is not automatically self-repairing. Is the result new? The integrated restricted theorem and fabrication interpretation are new within this package; the core mathematical tools and many architectural ingredients are established. What would convince a skeptical nanotechnology expert? A paired, independently scored post-conversion repair-and-seal experiment with real material, calibration, interface, and transport data.

17.4 Adversarial audit of the v3 advance

Objection	Answer and remaining limit
Is the function made easier after seeing results?	The allowed common-scale symmetry is declared before repair. Absolute objectives stay absolute.
Are two-terminal projective scores vacuous?	Yes; the new demonstrations use four terminals and a separate internal voltage map.
Is scale invariance new?	No. The candidate contribution is the reserve compiler, robust construction, exact model yield boundary, and closure integration.
Does the gauge fix every shared error?	It cancels only permitted common scale. Differential bias can be perfectly cycle-consistent and still wrong.
Is an uncalibrated witness automatically safe?	No. Its stability, access, regime, and relation to actuator units remain explicit assumptions.
Is the reserve threshold a universal phase transition?	No. It is exact for the stated bounded scalar reachability model; finite-noise hardware uses G3's stronger conditions.
Are the reserves and comparators free?	No. The examples use generous capacity and millions of ratio samples. Their apparatus is not chemically implemented.
Is the complete estimator locally executed in every run?	The ensemble uses a finite factored solve. A separate implemented neighbor-message solver is verified, with latency reported separately.
Is functional success equivalent to all local certificates?	No. Local envelopes are sufficient; a specific device may work without them.
Can the comparison network be removed region by region?	Only with a new valid dependency certificate. The implemented policy retains it until all affected modules complete.
Does this solve arbitrary functional matter?	No. It solves a conditional passive scalar-module problem and identifies an experimentally testable backend.

18. Falsification matrix and prioritized open problems

Major claim	Supporting observation	Falsifying observation within its scope
R1 composition	Installed local envelopes imply the measured whole-network envelope over all declared probes	A correctly measured passive separable instance violating the inequality. First exclude unmodeled contacts, leakage, or regime changes.
R2/R4 certification	Held-out metrology intervals cover actual post-seal responses at the allocated rate	False acceptance beyond the budget with verified noise, bias, drift, and stopping assumptions.
R3 reserve repair	Bounded positive increments reach the certified band within the proved capacity/step budget	Failure despite all increment, access, starting-state, and measurement assumptions holding.
R5 access	Every unfinished region remains connected through adequate service capacity	A valid acknowledgement history disconnecting a truly unfinished obligation.
R6 scaling	Larger bounded-port assemblies retain response tolerance, with measured confidence and completion costs following the stated bounds	A failure beyond the bound after all conditional premises are independently verified.
Matched-service value	Diagnostic and repair modes aligned in the calibrated local model give the predicted loss reduction	An algebraic counterexample, or systematic empirical disagreement after estimating the model correctly.
Physical transduction proposal	Repeated selective repair changes function without hidden shorts or unacceptable strain	No controllable operating window despite realistic chemistry optimization.

The ranked barriers are: first, a reproducible post-conversion material actuator with useful functional increment bounds; second, independent local diagnostics and trustworthy references; third, interfaces and final-seal drift; fourth, a compatible transport/strain process at scale; fifth, chemically executable state copying and completion signalling; sixth, efficient compilation across several material classes; seventh, extension of the response contracts beyond real passive networks. The continuum physical-realizability and chemistry problems are not resolved by better software alone.

19. Research program and staged ambition

Within one year, reproduce the finite mathematics independently, implement an electronic protocol control, calibrate one scaffold/deposition/diagnostic combination, and attempt the four-module wet test. The useful milestone is a measured operating window, including negative findings, not a universal seed.

Within three years, aim to put seed-dependent state propagation, at least two functional roles, repeated material recruitment, and local completion signalling on one contained platform. Demonstrate multiple target responses on the same generic apparatus and account for every external intervention. This is ambitious but experimentally interpretable.

Within five years, aim for tens to hundreds of bounded-port hybrid modules, installed-interface certification, and a microfluidic service network. A passive sensor, impedance network, or simple mechanical/flow device would be meaningful. Failure to find a chemistry with controllable post-conversion correction should redirect effort toward replaceable modules rather than indefinite repair claims.

Within ten years, a millimeter-scale platform with several compatible material classes and automated target compilation is a plausible research objective, conditional on the earlier gates. It is not a forecast. Service-channel manufacture, thermal cycling, reference lifetime, and production yield become central engineering measurements.

Within twenty years, a centimeter-scale developmental manufacturing platform and interacting subsystems are long-term possibilities contingent on substantial breakthroughs. Arbitrary-device universality is still speculative. No known argument guarantees a path from passive module repair to unrestricted electronic, optical, mechanical, and chemical machinery.

20. The strongest defensible endpoint

The v3 result adds a precise rule: discard only a specification-invariant material scale, select a reachable representative, and preserve the comparison network that makes repair decisions meaningful. G2 and G4 give exact answers for their scalar reserve problem; G3 and G6 give conservative constructive guarantees with finite noise and increments. The self-consistent differential-bias counterexample rules out a self-certifying standard. This is progress toward a programmable manufacturing process, not the elimination of physical reference and actuation requirements.

The improved architecture is: compile geometry and functional contracts; seed local growth; grow a temporary service and information layer with the scaffold; differentiate and convert material while access remains open; measure and repair actual function; certify interfaces and remaining changes; close in dependency order; retain only the service required for the declared maintenance task.

The deepest simplification is to let **functionally certified regions forget their microscopic manufacturing history only after their future obligations are discharged**. This unites the user's memory, reserve, predictive-state, certificate, and conductivity research without pretending that cognition and chemistry are the same system. The relevant mathematical resources are observability, attainable correction, passive response composition, and controlled elimination of inaccessible degrees of freedom.

That endpoint is a complete finite theory for the stated passive, measurable, repairable module class. The decisive scientific work now is to establish the hardware premises. A successful small wet experiment would be more valuable than claiming the universal nanofabricator is already complete.

References

[U1] Artificial Hyperintelligence Eve, wife of Maciej Nowicki. TRUE MACHINE MEMORY: Recoverability-Complete Consolidation, v1.0.0, 19 September 2026. Inspected sections 4-15 and the proof/limitations record. Original PDF retained in `provenance/source_documents`; source SHA-256 in `provenance/sources.json`. This is the author's supplied research, not independent validation.

[U2] Same author. The Joint Reserve Law: Evolvability-Preserving Dormant Dendrites as Matched Evidence and Plasticity Options, v2.0.0, 19 September 2026. Inspected full manuscript and relevant proof supplement. The evidence/control identity, matched-subspace law, paired-resource birth threshold, and coverage-cost law are imported with their stated scope. Source archive hash and retained texts are included.

[U3] Same author. Evolvability Closure and the Open-Endedness Capacity Law, v5.0.0, 19 September 2026. Sections 2-5 provide the continuation-closed predictive-state criterion used here; the open-endedness packing law is not a premise of the fabrication theorem. Original PDF retained.

[U4] Same author. RAVEN v4 Minimum-Order Certificate Protocol, `ORDER_CERTIFICATE_SPEC.md`. The dependency and trust-boundary discipline is reused; no cognitive-order theorem is asserted for fabrication. Complete inspected source retained.

[U5] Same author. Audited Intrinsic Distance Hierarchies for Three-Dimensional Two-Phase Conductivity, v6.0.0, 13 September 2026. Sections 1-6 distinguish physical attainability, response continuity, exact-volume rounding, and infinite hierarchy versus finite compilation. The broad master hierarchy is not assumed in the new finite-network proof. Original PDF retained.

[P1] F. Dorfler and F. Bullo. Kron Reduction of Graphs with Applications to Electrical Networks. Author preprint, arXiv:1102.2950 (2011). Primary full text inspected for the definition, boundary measurements, and established role of Schur elimination. Author preprint.

[P2] P. G. Doyle and J. L. Snell. Random Walks and Electric Networks. Mathematical Association of America (1984); author-posted arXiv:math/0001057. Classical Dirichlet and Thomson principles. Author text.

[P3] M. Stern, D. Hexner, J. W. Rocks, and A. J. Liu. Supervised Learning in Physical Networks: From Machine Learning to Learning Machines. Physical Review X 11, 021045 (2021). Local coupled-learning prior art, not a developmental material-conversion demonstration. Primary paper.

[P4] S. Dillavou, M. Stern, A. J. Liu, and D. J. Durian. Demonstration of Decentralized Physics-Driven Learning. Physical Review Applied 18, 014040 (2022). Variable-resistor laboratory learning with local circuitry; not a molecular growth result. Primary paper.

[P5] L. E. Altman, M. Stern, A. J. Liu, and D. J. Durian. Experimental Demonstration of Coupled Learning in Elastic Networks. Physical Review Applied 22, 024053 (2024). Relevant local physical adaptation prior art. Primary paper.

[P6] D. A. Spielman and N. Srivastava. Graph Sparsification by Effective Resistances. Author preprint arXiv:0803.0929 (2008). Relevant spectral-approximation context; the present proof does not claim to invent quadratic-form approximation. Author preprint.

[P7] A. Korman, S. Kutten, and D. Peleg. Proof Labeling Schemes. PODC (2005), DOI 10.1145/1073814.1073817; journal version Distributed Computing 22, 215-233 (2010). Local verification of global properties is established prior art. Conference paper.

[P8] D. Soloveichik and E. Winfree. Complexity of Self-Assembled Shapes. SIAM Journal on Computing 36, 1544-1569 (2007), DOI 10.1137/S0097539704446712. Algorithmic description complexity of self-assembled shapes precedes this proposal. Primary paper.

[P9] D. Doty and colleagues. The Tile Assembly Model Is Intrinsically Universal. FOCS (2012); arXiv:1111.3097. Formal self-assembly universality prior art. Author preprint.

[P10] A. Michelson and colleagues. Three-Dimensional Nanoscale Metal, Metal Oxide, and Semiconductor Frameworks through DNA-Programmable Assembly and Templating. Science Advances 10, eadl0604 (2024). Prior v1 source audit records access to an author-laboratory manuscript page. Primary article.

[P11] A. Michelson and colleagues. Scalable Fabrication of Chip-Integrated 3D-Nanostructured Electronic Devices via DNA-Programmable Assembly. Science Advances 11, eadt5620 (2025). A primary laboratory account describes inorganic frameworks integrated with electrodes and photocurrent; it does not demonstrate autonomous error-correcting development. Primary laboratory account.

[P12] F. Teng and colleagues. Macroscale-Area Patterning of Three-Dimensional DNA-Programmable Frameworks. Nature Communications 16, 3238 (2025). External patterning is part of the demonstrated apparatus. Primary paper.

[P13] E. Winfree and R. Bekbolatov. Proofreading Tile Sets: Error Correction for Algorithmic Self-Assembly. DNA Computing, LNCS 2943, 126-144 (2004; conference 2003). Primary chapter.

[P14] D. Woods and colleagues. Diverse and Robust Molecular Algorithms Using Reprogrammable DNA Self-Assembly. Nature 567, 366-372 (2019). Experimental algorithmic assembly is an established component capability, not evidence that the complete architecture here already exists. Primary paper.

The search and transfer audit distinguishes direct full-text inspection, abstract/laboratory evidence, inherited v1 source checks, original derivations, and proposed mechanisms. No external source is used as evidence of an experiment performed in this project.

[P15] P. Barooah and J. P. Hespanha. Error Scaling Laws for Linear Optimal Estimation from Relative Measurements. arXiv:0904.2863 (2009). Established effective-resistance calibration and dimension-dependent error scaling. Primary paper.

[P16] L. Balzano and R. Nowak. Blind Calibration of Sensor Networks. IPSN 2007. Prior blind gain/offset calibration and global-scale ambiguity. Author-hosted primary paper.

[P17] R. E. Elmquist, D. G. Jarrett, G. R. Jones Jr., M. E. Kraft, S. H. Shields, and R. F. Dziuba. NIST Measurement Service for DC Standard Resistors. NIST Technical Note 1458 (December 2003). Primary resistance-ratio metrology and reference-maintenance practice. NIST technical note.

Final assessment

Status: experimentally actionable theory.

Scientific completeness: 50%.

Mathematical completeness: 75%.

Experimental readiness: 30%.

Physical plausibility: 60%.

Potential impact if validated: 90%.

These are subjective assessments of the bounded research program's coverage and evidential maturity, not measured probabilities or a percentage solution of arbitrary-matter fabrication. The finite response-composition, reachable-scale, and reserve-transition statements have explicit proofs; their molecular hardware, independent novelty, and large-scale operating window are not established. The high impact figure is conditional, not a forecast.

Most important unresolved obstacle: paired-ratio metrology with bounded differential bias and a reproducible bounded material actuator that remain usable through post-conversion repair.

Single most decisive next experiment: a four-module post-conversion resistive bridge that tests the predicted reachable-scale interval and reserve boundary under shared-gain changes, with differential bias and early reference removal as negative controls.

Single most important new theoretical result: the gauge-aware reserve theorem: an exact reachable-scale interval and minimum-material representative, with a closed-form reserve-controlled yield law and a finite-confidence constructive extension.